

The Discovery reach of CP violation in neutrino oscillation with non-standard interaction effects

Zini Rahman,^{1,*} Arnab Dasgupta,^{1,†} and Rathin Adhikari^{1,‡}

¹*Centre for Theoretical Physics, Jamia Millia Islamia (Central University),
Jamia Nagar, New Delhi-110025, India*

We have studied the CP violation discovery reach in neutrino oscillation experiment with superbeam, neutrino factory and monoenergetic neutrino beam from electron capture process. For NSI satisfying model-dependent bound for shorter baselines (like CERN-Fréjus set-up) there is insignificant effect of NSI on the the discovery reach of CP violation due to δ . Particularly, for superbeam and neutrino factory we have also considered relatively longer baselines for which there could be significant NSI effects on CP violation discovery reach for higher allowed values of NSI. For monoenergetic beam only shorter baselines are considered to study CP violation with different nuclei as neutrino sources. Interestingly for non-standard interactions - $\varepsilon_{e\mu}$ and $\varepsilon_{e\tau}$ of neutrinos with matter during propagation in longer baselines in superbeam, there is possibility of better discovery reach of CP violation than that with only Standard Model interactions of neutrinos with matter. For complex NSI we have shown the CP violation discovery reach in the plane of Dirac phase δ and NSI phase ϕ_{ij} . The CP violation due to some values of δ remain unobservable with present and near future experimental facilities in superbeam and neutrino factory . However, in presence of some ranges of off-diagonal NSI phase values there are some possibilities of discovering total CP violation for any δ_{CP} value even at 5σ confidence level for neutrino factory. Our analysis indicates that for some values of NSI phases total CP violation may not be at all observable for any values of δ . Combination of shorter and longer baselines could indicate in some cases the presence of NSI. However, in general for NSIs $\lesssim 1$ the CP violation discovery reach is better in neutrino factory set-ups. Using a neutrino beam from electron capture process for nuclei $^{110}_{50}\text{Sn}$ and ^{152}Yb , we have shown the discovery reach of CP violation in neutrino oscillation experiment. Particularly for $^{110}_{50}\text{Sn}$ nuclei CP violation could be found for about 51% of the possible δ values for a baseline of 130 km with boost factor $\gamma = 500$. The nuclei ^{152}Yb is although technically more feasible for the production of mono-energetic beam, but is found to be not suitable in obtaining good discovery reach of CP violation.

* zini@ctp-jamia.res.in

† arnab@ctp-jamia.res.in

‡ rathin@ctp-jamia.res.in

I. INTRODUCTION

Long back CP violation has been found in the quark sector of the Standard Model of Particle Physics. But so far there is no evidence of CP violation in the leptonic sector. One way to search for such CP violation is through neutrino oscillation experiments in which one flavor of neutrino could oscillate to other flavors of neutrinos. Neutrino oscillation probability depends on various oscillation parameters present in the 3×3 mixing matrix - the PMNS matrix [1–3] and the neutrino mass squared differences. Two of the three angles - θ_{12} and θ_{23} present in PMNS matrix have been known with certain accuracy for some time. Recently several experiments like Double CHOOZ, Daya Bay, RENO and T2K collaboration [4–7] found non-zero value of $\sin^2 2\theta_{13}$ corresponding to the third mixing angle of PMNS matrix with a global level of significance which is well above conventional 5σ discovery threshold. As three angles are non-zero there could be non-zero CP violating phase δ in the PMNS matrix and as such there could be CP violation in the leptonic sector. The mass squared differences - $|\Delta m_{31}^2|$ and Δm_{21}^2 is known (where $\Delta m_{ij}^2 = m_i^2 - m_j^2$) but the sign of Δm_{31}^2 and as such the hierarchy (whether it is normal (NH) or inverted (IH)) of neutrino masses is still unknown. Various neutrino oscillation experiments like superbeam, neutrino factory, beta beams and reactor experiments are focussing on determining these unknown parameters corresponding to neutrino oscillations [8–19].

There could be various kind of non-standard interactions of neutrinos with matter. This could have some effect on finding CP violation in neutrino oscillation experiments. Such interactions could be the non-standard interactions of neutrinos with matter fermions (u, d and e) during propagation of neutrinos only. This could affect oscillations of different flavors of neutrinos as sub-leading effect. We have discussed it in further detail in the next section. There could be other different kind of interactions beyond Standard model leading to non-unitarity of 3×3 PMNS neutrino mixing matrix [20]. Considering non-standard interactions of neutrinos at the source and the detector in neutrino oscillation experiments also lead to such possibility. However, such NSI at the source and detector have highly stringent constraints [21] and as such the effect on neutrino oscillation is expected to be lesser affected than that due to NSI in matter during propagation of neutrinos. We shall not consider NSI at the source and detector in this work.

To study CP violation in neutrino oscillation experiments we have considered superbeam, neutrino factory and monoenergetic neutrino beam from electron capture process. There are some earlier studies for short and long baselines for standard interactions [18, 19, 22–26] for neutrinos coming from superbeam. We consider neutrino superbeam (which mainly contains ν_μ and $\bar{\nu}_\mu$) coming from CERN travelling a baseline length of 2300 km to Pyhäsalmi (Finland) and another baseline of 130 km to Fréjus (France). We have also considered superbeam coming from Tokai to Hyper-Kamiokande travelling a baseline of 295 km. We do a comparative study in the discovery potentials of the CP violating phase δ for these three baselines in presence of both standard and non-standard interactions. Main emphasis of our work is on exploring CP violation due to δ in the light of recent experimental findings of large value of θ_{13} and how NSI could affect the discovery reach of such CP violation. Also there are some studies on CP violation in presence of non-standard interactions [27, 28] before Daya Bay experiment when θ_{13} was not so precisely known.

The discovery of CP violation for different parent muon energy in neutrino factory and different length of baselines have been studied earlier [29, 30]. In the analysis done in [29] three different kinds of magnetized detectors: a Totally-Active Scintillator (TASD) and two kinds of Liquid Argon detectors have been considered for baselines ranging from 1000 km to 4000 km and parent muon energies from 4 GeV to 25 GeV, whereas in the analysis done in [30] MIND (Toroidal magnetized iron neutrino detector) detector has been considered. As recent reactor neutrino experiments indicates large value of θ_{13} it is important to study the discovery

potential of CP violation in neutrino oscillation experiments in low energy neutrino factory [31]. There are some studies on the performance of low energy neutrino factories [15] in the context of standard model interactions of neutrinos with matter [29, 31–38] and also in presence of NSI [39–43]. In the works related to NSI [39–43] longer baselines like 4000 and 7500 kms has been considered to have larger NSI effect on neutrino oscillation experiments so as to find better NSI sensitivity and in that context CP violation has also been studied.

Our work is complementary to these earlier analysis in the sense that we focus here on the better discovery reach of CP violation and as such we consider relatively shorter baselines where the matter effect and as such NSI effect will be lesser in the neutrino oscillation experiments. However, in the context of such experimental set-up in neutrino factory which is better optimized for CP violation discovery (considering only SM interactions of neutrinos with matter) we have also addressed the question of CP violation coming due to NSI phases. We have considered lower parent muon energy within 10 GeV which is found to be more favourable for the discovery of CP violation. The optimization for CP violation discovery in the context of SM interactions has been done earlier [29, 30]. However, in this work we re-analysed this optimization with the updated detector characteristics for the MIND detector [44]. Based on this optimization we have chosen a few relatively shorter baselines (730, 1290 and 1500 kms) and low parent muon energy of 10 GeV.

In recent years oscillation experiment using a neutrino beam with neutrinos emitted from an electron capture process is proposed [16, 45–51]. Such beam can be produced using an accelerated nuclei that decay by electron capture. In this process an electron is captured by a proton releasing a neutron and an electron neutrino. So the beam is purely of one flavor. In the rest frame of the mother nuclei the electron neutrino that is released from such process, has a definite energy Q . Since the idea of using a neutrino beam emitted from an electron capture process is based on the acceleration and storage of radioactive isotopes that decays to daughter nuclei, one may get the suitable neutrino energy by accelerating the mother nuclei with suitable Lorentz boost factor γ . One can control the neutrino energy by choosing the appropriate Lorentz boost factor as the energy that has been boosted by an appropriate boost factor towards the detector is given as $E = 2\gamma Q$. Hence for certain mother nuclei to get the required neutrino energy the boost factor have to be chosen appropriately with respect to Q . Due to the almost monoenergetic nature of such beam one can appropriately choose the neutrino energy for which the probability of oscillation could be large and sensitive to certain unknown neutrino oscillation parameters.

In this work we consider such a flavor pure electron neutrino beam emitted from electron capture process for a suitable γ value where the beam is targeted towards a Water Cherenkov detector and perform numerical simulation to study the discovery reach of CP violation in oscillation experiments.

In section II we have mentioned various model dependent and independent bounds of NSIs and have discussed the neutrino oscillation probability in presence of NSI. In section III, we have discussed the procedure of numerical simulation and in its different subsections related to superbeam, neutrino factory and monoenergetic neutrino beam we have discussed various experimental set-ups and results of our analysis on discovery of CP violation. In section IV we have concluded with some remarks on the possibility of knowing the presence of NSIs in the context of superbeam and neutrino factory. For monoenergetic beam we have discussed the suitable nuclei for discovering CP violation and related technical constraints.

II. NSI AND ITS EFFECT ON NEUTRINO OSCILLATION PROBABILITIES

We consider the non-standard interactions of neutrinos which could be outcome of effective theory at low energy after integrating out the heavy mediator fields at the energy scale of neutrino oscillation experiments. Apart from Standard Model (SM) Lagrangian density we consider the following non-standard fermion-neutrino interaction in matter defined by the Lagrangian:

$$\mathcal{L}_{NSI}^M = -2\sqrt{2}G_F\varepsilon_{\alpha\beta}^{fP}[\bar{f}\gamma_\mu Pf][\bar{\nu}_\beta\gamma^\mu L\nu_\alpha] \quad (1)$$

where $P \in (L, R)$, $L = \frac{(1-\gamma^5)}{2}$, $R = \frac{(1+\gamma^5)}{2}$, $f = e, u, d$ and $\varepsilon_{\alpha\beta}^{fP}$ are termed as non-standard interactions (NSIs) parameters signifying the deviation from SM interactions. These are non-renormalizable as well as not gauge invariant and are dimension-6 operators after heavy fields are integrated out [21]. Although at low energy NSI look like this but at high energy scale where actually such interactions originate there they have different form. These NSI parameters can be reduced to the effective parameters and can be written as:

$$\varepsilon_{\alpha\beta} = \sum_{f,P} \varepsilon_{\alpha\beta}^{fP} \frac{n_f}{n_e} \quad (2)$$

where n_f and n_e are the fermion and the electron number density respectively in matter. As these NSIs modify the interactions with matter from the Standard Model interactions the effective mass matrix for the neutrinos are changed and as such there will be change in the oscillation probability of different flavor of neutrinos. Although NSIs could be present at the source of neutrinos, during the propagation of neutrinos and also during detection of neutrinos [52] but as those effects are expected to be smaller at the source and detector due to their stringent constraints [21, 53], we consider the NSI effect during the propagation of neutrinos only.

Model dependent [21, 54–66] and independent [53, 67, 68] bounds are obtained for these matter NSI parameters and are shown in the following table. In obtaining model dependent bounds on matter NSI the experiments with neutrinos and charged leptons - LSND, CHARM, CHARM-II, NuTeV and also LEP-II have been considered. Bounds coming from loop effect have been used for model dependent bounds. However, model independent bounds are less stringent and could be larger than the model dependent bounds by several orders and have been discussed in [21, 53]. Considering recent results from experiments in IceCube-79 and

NSI	Model dependent bound on NSI [Reference [21]]	Model independent Bound on NSI [Reference [53]]
ε_{ee}	$> -0.9; < 0.75$	< 4.2
$ \varepsilon_{e\mu} $	$\lesssim 3.8 \times 10^{-4}$	< 0.33
$ \varepsilon_{e\tau} $	$\lesssim 0.25$	< 3.0
$\varepsilon_{\mu\mu}$	$> -0.05; < 0.08$	< 0.068
$ \varepsilon_{\mu\tau} $	$\lesssim 0.25$	< 0.33
$\varepsilon_{\tau\tau}$	$\lesssim 0.4$	< 21

TABLE I: Strength of Non standard interaction terms used for our Analysis.

DeepCore more stringent bound on $\varepsilon_{\mu\mu}$, $|\varepsilon_{\mu\tau}|$ and $\varepsilon_{\tau\tau}$ have been obtained in [68]. In section IV, we shall consider both model dependent and independent allowed range of values of different NSIs as shown in the table above for earth like matter while showing discovery reach for CP violation in presence of NSI.

A. $\nu_e \rightarrow \nu_\mu$ oscillation probabilities with NSI

The flavor eigenstates ν_α is related to mass eigenstates of neutrinos ν_i as

$$\nu_\alpha = \sum_i U_{\alpha i} \nu_i ; \quad i = 1, 2, 3, \quad (3)$$

in vacuum where U is 3×3 unitary matrix parametrized by three mixing angles θ_{12} , θ_{23} and θ_{13} and by one CP violating phase δ for Dirac neutrino as given in [2, 3]. However, for Majorana neutrino apart from δ there are two more CP violating phases which do not play role in neutrino oscillation [2].

In the flavor basis the total Hamiltonian consisting both standard (H_{SM}) and non-standard interactions (H_{NSI}) of neutrinos interacting with matter during propagation can be written as:

$$H = H_{SM} + H_{NSI} \quad (4)$$

where

$$H_{SM} = \frac{\Delta m_{31}^2}{2E} \left[U \begin{pmatrix} 0 & 0 & 0 \\ 0 & \alpha & 0 \\ 0 & 0 & 1 \end{pmatrix} U^\dagger + \begin{pmatrix} A & 0 & 0 \\ 0 & 0 & 0 \\ 0 & 0 & 0 \end{pmatrix} \right], \quad (5)$$

$$H_{NSI} = \frac{\Delta m_{31}^2}{2E} A \begin{pmatrix} \varepsilon_{ee} & \varepsilon_{e\mu} & \varepsilon_{e\tau} \\ \varepsilon_{e\mu}^* & \varepsilon_{\mu\mu} & \varepsilon_{\mu\tau} \\ \varepsilon_{e\tau}^* & \varepsilon_{\mu\tau}^* & \varepsilon_{\tau\tau} \end{pmatrix} \quad (6)$$

In equations (5) and (6)

$$A = \frac{2E\sqrt{2}G_F n_e}{\Delta m_{31}^2}; \quad \alpha = \frac{\Delta m_{21}^2}{\Delta m_{31}^2}; \quad \Delta m_{ij}^2 = m_i^2 - m_j^2 \quad (7)$$

where m_i is the mass of the i -th neutrino, A corresponds to the interaction of neutrinos with matter in SM and G_F is the Fermi constant. ε_{ee} , $\varepsilon_{e\mu}$, $\varepsilon_{e\tau}$, $\varepsilon_{\mu\mu}$, $\varepsilon_{\mu\tau}$ and $\varepsilon_{\tau\tau}$ correspond to the non-standard interactions (NSIs) of neutrinos with matter. In equation (6), (*) denotes complex conjugation. The NSIs - $\varepsilon_{e\mu}$, $\varepsilon_{e\tau}$ and $\varepsilon_{\mu\tau}$ could be complex. Later on, in the expressions of probability of oscillation we have expressed these NSIs as $\varepsilon_{ij} = |\varepsilon_{ij}|e^{i\phi_{ij}}$. In our numerical analysis we have considered the NSIs - $\varepsilon_{e\mu}$, $\varepsilon_{e\tau}$ and $\varepsilon_{\mu\tau}$ as both real as well as complex.

For longer baselines following the perturbation method adopted in references [69, 70] for the oscillation probability $P_{\nu_e \rightarrow \nu_\mu}$ upto order α^2 (considering $\sin \theta_{13} \sim \sqrt{\alpha}$ as follows from recent reactor experiments) and the matter effect parameter A in the leading order of perturbation (which happens for longer baselines) and NSI parameters $\varepsilon_{\alpha\beta}$ of the order of α one obtains [71]

$$P_{\nu_e \rightarrow \nu_\mu} = P_{\nu_e \rightarrow \nu_\mu}^{SM} + P_{\nu_e \rightarrow \nu_\mu}^{NSI} \quad (8)$$

where

$$\begin{aligned} P_{\nu_e \rightarrow \nu_\mu}^{SM} &= 4 \sin \frac{(A-1)\Delta m_{31}^2 L}{4E} \frac{s_{13}^2 s_{23}^2}{(A-1)^4} \left(((A-1)^2 - (1+A)^2 s_{13}^2) \sin \frac{(A-1)\Delta m_{31}^2 L}{4E} \right. \\ &+ A(A-1) \frac{\Delta m_{31}^2 L}{E} s_{13}^2 \cos \frac{(A-1)\Delta m_{31}^2 L}{4E} \left. \right) + \frac{\alpha^2 c_{23}^2}{A^2} \sin^2 2\theta_{12} \sin^2 \frac{\Delta m_{31}^2 AL}{4E} \\ &+ \frac{\alpha s_{12}^2 s_{13}^2 s_{23}^2}{(A-1)^3} \left(\frac{(A-1)\Delta m_{31}^2 L}{E} \sin \frac{(A-1)\Delta m_{31}^2 L}{2E} - 8A \sin^2 \frac{(A-1)\Delta m_{31}^2 L}{4E} \right) \\ &+ \frac{\alpha s_{13} s_{2 \times 12} s_{2 \times 23}}{A(A-1)} \left(2 \cos \left(\delta - \frac{\Delta m_{31}^2 L}{4E} \right) \sin \frac{(A-1)\Delta m_{31}^2 L}{4E} \sin \frac{A\Delta m_{31}^2 L}{4E} \right) \end{aligned} \quad (9)$$

$$\begin{aligned} P_{\nu_e \rightarrow \nu_\mu}^{NSI} &= \frac{4|a_2|s_{2 \times 23}s_{13}}{A(A-1)} \sin \frac{A\Delta m_{31}^2 L}{4E} \sin \frac{(A-1)\Delta m_{31}^2 L}{4E} \cos \left(\delta - \frac{\Delta m_{31}^2 L}{4E} + \phi_{a_2} \right) \\ &+ \frac{4|a_3|s_{23}^2}{(A-1)^2} \sin^2 \frac{(A-1)\Delta m_{31}^2 L}{4E} (|a_3| + 2 \cos(\delta + \phi_{a_3})s_{13}) \\ &+ \frac{s_{13}^2 s_{23}^2 (|a_5| - |a_1|)}{(A-1)^3 E} \left(8E \sin^2 \frac{(A-1)\Delta m_{31}^2 L}{4E} - (A-1)\Delta m_{31}^2 L \sin \frac{(A-1)\Delta m_{31}^2 L}{2E} \right) \\ &+ \frac{4|a_2|c_{23}}{(A-1)A^2} \sin \frac{A\Delta m_{31}^2 L}{4E} \left((A-1)c_{23} \sin \frac{A\Delta m_{31}^2 L}{4E} (|a_2| + \alpha \cos \phi_{a_2} \sin 2\theta_{12}) \right) \\ &- \frac{4|a_2||a_3| \sin 2\theta_{23}}{A(A-1)} \cos \left[\frac{\Delta m_{31}^2 L}{4E} - \phi_{a_2} + \phi_{a_3} \right] \sin \frac{(1-A)\Delta m_{31}^2 L}{4E} \sin \frac{A\Delta m_{31}^2 L}{4E} \\ &+ \frac{4|a_3|s_{23}}{(A-1)^2 A} \sin \frac{(A-1)\Delta m_{31}^2 L}{4E} (A-1)\alpha c_{23} \cos \left[\frac{\Delta m_{31}^2 L}{4E} - \phi_{a_3} \right] \sin \frac{A\Delta m_{31}^2 L}{4E} \sin 2\theta_{12} \\ &+ \frac{|a_4|s_{13}^2 \sin 2\theta_{23}}{(A-1)^2 A} \sin \frac{(A-1)\Delta m_{31}^2 L}{4E} \left(-4A \cos \frac{A\Delta m_{31}^2 L}{4E} \cos \phi_{a_4} \sin \frac{\Delta m_{31}^2 L}{4E} \right. \\ &\left. + 4 \sin \frac{A\Delta m_{31}^2 L}{4E} \left(\cos \frac{\Delta m_{31}^2 L}{4E} \cos \phi_{a_4} + (A-1) \sin \frac{\Delta m_{31}^2 L}{4E} \sin \phi_{a_4} \right) \right) \end{aligned} \quad (10)$$

where

$$\begin{aligned}
a_1 &= A\varepsilon_{ee} \\
|a_2|e^{i\phi_{a_2}} &= A\left(e^{i\phi_{e\mu}}|\varepsilon_{e\mu}|c_{23} - e^{i\phi_{e\tau}}|\varepsilon_{e\tau}|s_{23}\right) \\
|a_3|e^{i\phi_{a_3}} &= A\left(e^{i\phi_{e\tau}}|\varepsilon_{e\tau}|c_{23} + e^{i\phi_{e\mu}}|\varepsilon_{e\mu}|s_{23}\right) \\
|a_4|e^{i\phi_{a_4}} &= A\left(|\varepsilon_{\mu\tau}|e^{i\phi_{\mu\tau}} - 2|\varepsilon_{\mu\tau}|s_{23}^2 + (\varepsilon_{\mu\mu} - \varepsilon_{\tau\tau})c_{23}s_{23}\right) \\
a_5 &= A\left(\varepsilon_{\tau\tau}c_{23}^2 + \varepsilon_{\mu\mu}s_{23}^2 + |\varepsilon_{\mu\tau}|\cos\phi_{\mu\tau}s_{2\times 23}\right)
\end{aligned} \tag{11}$$

and

$$\begin{aligned}
\phi_{a_2} &= \tan^{-1} \left[\frac{|\varepsilon_{e\mu}|c_{23} \sin\phi_{e\mu} - |\varepsilon_{e\tau}|s_{23} \sin\phi_{e\tau}}{|\varepsilon_{e\mu}|c_{23} \cos\phi_{e\mu} - |\varepsilon_{e\tau}| \cos\phi_{e\tau}s_{23}} \right] \\
\phi_{a_3} &= \tan^{-1} \left[\frac{|\varepsilon_{e\mu}|s_{23} \sin\phi_{e\mu} + |\varepsilon_{e\tau}|c_{23} \sin\phi_{e\tau}}{|\varepsilon_{e\tau}|c_{23} \cos\phi_{e\tau} + |\varepsilon_{e\mu}| \cos\phi_{e\mu}s_{23}} \right] \\
\phi_{a_4} &= \tan^{-1} \left(\frac{|\varepsilon_{\mu\tau}| \sin(\phi_{\mu\tau})}{|\varepsilon_{\mu\tau}|c_{2\times 23} \cos(\phi_{\mu\tau}) + (\varepsilon_{\mu\mu} - \varepsilon_{\tau\tau})c_{23}s_{23}} \right)
\end{aligned} \tag{12}$$

where $s_{ij} = \sin\theta_{ij}$, $c_{ij} = \cos\theta_{ij}$, $s_{2\times ij} = \sin 2\theta_{ij}$, $c_{2\times ij} = \cos 2\theta_{ij}$. The oscillation channel $\nu_e \rightarrow \nu_\mu$ is important for neutrino factory. For superbeam, $\nu_\mu \rightarrow \nu_e$ oscillation channel is important which can be obtained by the following transformation

$$P_{\alpha\beta}(A, \delta, \phi_{ij}) = P_{\beta\alpha}(A, -\delta, -\phi_{ij}). \tag{13}$$

The oscillation probabilities for antineutrinos can be obtained from the oscillation probabilities given for neutrinos above by using the following relation:

$$P_{\bar{\alpha}\bar{\beta}}(\delta, A, \phi_{ij}) = P_{\alpha\beta}(-\delta, -A, -\phi_{ij}). \tag{14}$$

To estimate the order of magnitude of δ dependent and δ independent but matter dependent (i.e., A dependent) part in the above two oscillation probability, following results of reactor experiments we shall consider $\sin\theta_{13} \sim \sqrt{\alpha}$. For only SM interactions, (i.e $\varepsilon_{\alpha\beta} \rightarrow 0$) from last term of Eq.(9) for oscillation probabilities one finds that the δ dependence occurs at order of $\alpha s_{13} \sim \alpha^{3/2}$ for both neutrino oscillation and anti-neutrino oscillation probabilities.

In presence of NSI of order α , in the first two leading terms of Eq.(10), the δ dependence occurs at order of $a_2 s_{13} \sim a_3 s_{13} \sim \alpha^{3/2}$ through terms containing a_2 and a_3 (which are $\varepsilon_{e\mu}$ and $\varepsilon_{e\tau}$ dependent). Due to this (if we assume all NSI of same order $\sim \alpha$), these two NSI ($\varepsilon_{e\mu}$ and $\varepsilon_{e\tau}$) in contrast to other NSI could have greater effect on oscillation probability in $\nu_e \rightarrow \nu_\mu$ or the reverse oscillation channel .

For shorter baselines the above oscillation probability expression becomes much simpler. Following the perturbation method [52] and by considering the standard model matter effect $A \sim \alpha$ for neutrino energy E around 1 GeV and $\sin \theta_{13} \sim \sqrt{\alpha}$ as obtained from reactor oscillation data, the probability of oscillation $P_{\nu_e \rightarrow \nu_\mu}$ upto order α^2 is given by

$$P_{\nu_e \rightarrow \nu_\mu} = P_{\nu_e \rightarrow \nu_\mu}(\alpha) + P_{\nu_e \rightarrow \nu_\mu}(\alpha^{3/2}) + P_{\nu_e \rightarrow \nu_\mu}(\alpha^2) \quad (15)$$

where

$$\begin{aligned} P_{\nu_e \rightarrow \nu_\mu}(\alpha) &= \sin^2 2\theta_{13} \sin^2 \theta_{23} \sin^2 \left(\frac{\Delta m_{31}^2 L}{4E} \right) \\ P_{\nu_e \rightarrow \nu_\mu}(\alpha^{3/2}) &= \alpha \left(\frac{\Delta m_{31}^2 L}{2E} \right) \sin \theta_{13} \sin 2\theta_{23} \sin 2\theta_{12} \sin \left(\frac{\Delta m_{31}^2 L}{4E} \right) \cos \left(\delta - \frac{\Delta m_{31}^2 L}{4E} \right) \\ P_{\nu_e \rightarrow \nu_\mu}(\alpha^2) &= \alpha^2 \cos^2 \theta_{23} \sin^2 2\theta_{12} \left(\frac{\Delta m_{31}^2 L}{4E} \right)^2 - 2\alpha \sin^2 \theta_{13} \sin^2 \theta_{12} \sin^2 \theta_{23} \frac{\Delta m_{31}^2 L}{2E} \sin \frac{\Delta m_{31}^2 L}{2E} \\ &\quad + 8A \sin^2 \theta_{13} \sin^2 \theta_{23} \left(\sin^2 \frac{\Delta m_{31}^2 L}{4E} - \frac{\Delta m_{31}^2 L}{8E} \sin \frac{\Delta m_{31}^2 L}{2E} \right) \end{aligned} \quad (16)$$

One may note that this expression of oscillation probability is little bit different from that presented by earlier authors [72] because they have considered the perturbative approach for relatively longer baseline and small $\sin \theta_{13} \sim \alpha$. For shorter baseline as presented here, the δ dependence appears to be more and instead of being at the order of α^2 it appears at the order $\alpha^{3/2}$ as $\alpha \sin \theta_{13} \sim \alpha^{3/2}$ although the expression is same. However at order α^2 some extra terms appear in comparison to that presented by earlier authors although their contribution is relatively smaller being at the order of α^2 . The matter effect is occurring at order α^2 through term containing parameter A .

III. NUMERICAL SIMULATION

There is detailed global analysis of three flavor neutrino oscillation data [73] presented at the *Neutrino 2012* conference. In their analysis the correlation between various oscillation parameters has been taken into account. Very recently there is another such global analysis [74] presented at the *Neutrino 2014* conference which has been considered in our analysis and best fit values of neutrino mixing parameters and their respective errors at 3σ confidence level are shown in table II. For earth matter density the PREM profile [75] has been considered. Also we have considered an error of 2% on matter density profile.

Oscillation Parameters	Central Values	Error (3σ)
$\frac{\Delta m_{21}^2}{10^{-5}} \text{ eV}^2$	7.45	7.02 - 8.09
$\frac{\Delta m_{31}^2}{10^{-3}} \text{ eV}^2$	2.457	2.325 - 2.599 (NH) (-2.59) - (-2.307) (IH)
$\sin^2 \theta_{12}$	0.304	0.270 - 0.344
$\sin^2 \theta_{23}$	0.452	0.385 - 0.644
$\sin^2 \theta_{13}$	0.0218	0.0188 - 0.0251

TABLE II: Central values of the oscillation parameters with errors.

The numerical simulation has been done by using GLoBES [76, 77]. GLoBES uses poissonian χ^2 for the oscillation parameters λ and for nuisance parameters ξ_i . To implement the systematic errors the ‘pull method’ [78] has been used by GLoBES and χ_{pull}^2 is given as [77]

$$\chi_{pull}^2(\lambda) := \min_{\{\xi_i\}} \left(\chi^2(\lambda, \xi_1, \dots, \xi_k) + \sum_{j=1}^k \frac{\xi_j^2}{\sigma_{\xi_j}^2} \right) \quad (17)$$

where $\chi^2(\lambda, \xi_1, \dots, \xi_n)$ is the usual Poissonian χ^2 depending on the neutrino oscillation parameters λ and the nuisance parameter ξ_i and it has been summed over different energy binning on the theoretical and observed event rates. The oscillation parameters λ is

$$\lambda = (\theta_{12}, \theta_{13}, \theta_{23}, \Delta m_{21}^2, \Delta m_{31}^2, \rho, \delta_{CP}, \varepsilon_{\alpha\beta}, \phi_{\alpha\beta}) ; \quad (18)$$

The nuisance parameters ξ_i are the signal and background normalization and the calibration errors. In order to implement the error σ_{ξ_i} , the χ^2 (in which all event rates of all bins are included) is minimized over the different nuisance parameters ξ_i independently.

We have also marginalized over λ' where

$$\lambda' = (\theta_{12}, \theta_{13}, \theta_{23}, \Delta m_{21}^2, \Delta m_{31}^2, \rho) . \quad (19)$$

The final projected χ_F^2 is given as

$$\chi_F^2 = \min_{\lambda'} (\chi_{pull}^2(\lambda) + \text{priors}(\lambda')) \quad (20)$$

where

$$\text{priors}(\lambda') = \left(\frac{\rho - \rho^0}{\sigma_\rho} \right)^2 + \sum_{i \neq j} \left(\frac{\sin^2 \theta_{ij} - \sin^2 \theta_{ij}^0}{\sigma_{\sin^2 \theta_{ij}}} \right)^2 + \left(\frac{\Delta m_{21}^2 - (\Delta m_{21}^2)^0}{\sigma_{\Delta m_{21}^2}} \right)^2 + \left(\frac{|\Delta m_{31}^2| - |(\Delta m_{31}^2)^0|}{\sigma_{|\Delta m_{31}^2|}} \right)^2 \quad (21)$$

and ρ^0 , $\sin^2 \theta_{12}^0$, $\sin^2 \theta_{13}^0$, $\sin^2 \theta_{23}^0$, $(\Delta m_{21}^2)^0$ and $|(\Delta m_{31}^2)^0|$ are the central values of the corresponding parameters. We have marginalized over two different hierarchies of neutrino masses also.

For taking into account NSI in GLoBES we have followed the method described in [77] and modified the source file “probability.c” in GLoBES appropriately by inserting the NSI’s in the subroutine where the hamiltonian for matter interaction is defined. Then we have included the new probability program as instructed by the manual of GLoBES. We have not used the approximate analytical expression of oscillation probability for NSI of order α in our numerical analysis.

At present we do not know the hierarchy of neutrino masses and the value of δ . In the test values we have considered both possibilities of the hierarchy. However, we shall show the results in Figures only for true normal hierarchy. Before we get the knowledge of specific value of δ it could be possible to know whether nature admits CP violation or not which could be possible for a wide range of values of δ . So what we are going to analyse is not the measurement of δ values but finding out all possible δ (true) values which could be distinguishable from the CP conserving δ values at certain confidence level through oscillation experiments. For that it is useful to calculate the CP fraction due to δ denoted as $F(\delta)$ which may be defined as the

fraction of the total allowed range (0 to 2π) for the $\delta(\text{true})$ over which CP violation can be discovered [29, 40]. While calculating the fraction due to δ for the discovery of CP violation, we consider the exclusion of all parameter sets with $\delta \in \{0, \pi\}$ which means $\delta(\text{test})$ is fixed in its CP conserving values $\{0, \pi\}$. For no NSIs, the degrees of freedom in χ^2 analysis is one due to δ . We have calculated the minimum of those χ^2 for each $\delta(\text{true})$ and have calculated the fraction of the $\delta(\text{true})$ over its entire range which satisfies $\Delta\chi^2 \geq 9(25)$ at $3(5)\sigma$ confidence level.

In studying the NSI effect (one at a time) on CP violation we have fixed absolute values of $\text{NSI}(\text{test})$ to their true values which implies that the absolute values of NSI are assumed to be known from some other experiments. In Figures we have shown the effect of real NSI's on the CP fraction discovery. In this case, the degrees of freedom in χ^2 analysis is one due to δ . The off-diagonal NSI in NSI matrix could be complex and the corresponding complex phases could be new sources of CP violation. If the CP violation is only due to NSI phase, then the CP fraction due to NSI phases ϕ_{ij} (denoted as $F(\phi_{ij})$) is calculated in the same way as described above for δ by replacing δ by the corresponding ϕ_{ij} . Here the degrees of freedom is one due to ϕ_{ij} . In Figures we have shown the effect of absolute values of non-diagonal NSI's (one at a time) on $F(\phi_{ij})$. In order to calculate the total CP violation discovery due to two phases ϕ_{ij} and δ we have set $\phi_{ij}(\text{test})$ and $\delta(\text{test})$ to their respective CP conserving values at $(\delta, \phi_{ij}) \in \{(0, 0), (0, \pi), (\pi, 0), (\pi, \pi)\}$ and also both of the mass hierarchy in the test values have been taken into account. Here, the degrees of freedom is two due to δ and one of the NSI phases ϕ_{ij} . Then we have calculated the above χ^2 minimum for each true values of ϕ_{ij} and δ and have shown the allowed region for discovery in ϕ_{ij} - δ space for $\Delta\chi^2 \geq 11.83$ at 3σ confidence level. In all Figures true hierarchy has been considered to be normal.

So by numerical simulation we are studying the different possibilities of finding CP violation in different experimental set-ups due to δ or NSI phase ϕ_{ij} or total CP violation due to δ and NSI phase ϕ_{ij} for certain absolute value of NSI ($\varepsilon_{ij}(\text{true})$) assumed to be present in nature. If we assume that any allowed values of δ has equal probability to be true δ value of nature then lower (higher) CP fraction which we present in the result sections will indicate lower (higher) probability of finding CP violation in particular experimental-set-up discussed below. One may note that NSI effect and the δ effect in the hamiltonian H has different neutrino energy dependence (see equation Eq.(5) for δ present in U and Eq.(6) for NSI). Also in the shorter (longer) baseline there should be lesser (larger) NSI effect. If the experimental data is available over certain range of neutrino energy from the shorter and longer baseline experiments then only the multi-parameter fit will help in disentangling effects due to different unknown parameters and hence improving bounds on NSI parameters or discovering it.

In the following we present three subsections based on three different sources of neutrino flux : Superbeam in III A, Neutrino Factory in III B and monoenergetic neutrino beam in III C. Particularly for Superbeam and Neutrino factory, we have studied the NSI effect in CP violation discovery in the leptonic sector in neutrino oscillation experiments. Monoenergetic neutrino beam requires shorter baseline due to technical reasons as discussed later. Due to that the NSI effect in the monoenergetic neutrino beam studies is insignificant and we will be discussing only CP violation discovery reach in absence of NSI. Two different nuclei have been considered for monoenergetic beam and to study CP violation.

A. Superbeam

We discuss below the experimental set-up and systematic errors for superbeam. We have presented our results for discovery reach of CP violation due to δ and other off-diagonal NSI phases ϕ_{ij} for different experimental set-up with different baselines. We have shown also the effect of the absolute values of different $\varepsilon_{\alpha\beta}$ in CP fraction.

1. Experimental set-ups and systematic errors

We consider three experimental set-ups: (a) A Superbeam set-up originating in CERN and reaching a 500 kt Water Cherenkov detector [79] placed at a distance of 130 km at Fréjus (France), (b) A Superbeam set-up originating in Tokai and reaching a 500 kt Water Cherenkov detector [13, 80, 81] placed at a distance of 295 km at Kamiokande (Japan) and (c) A Superbeam set-up which originates in CERN and reaches a 100 kt Liquid Argon detector placed at a distance of 2300 km at Pyhäsalmi (Finland). The observable channels that we have considered are $\nu_\mu \rightarrow \nu_e$, $\bar{\nu}_\mu \rightarrow \bar{\nu}_e$, $\nu_\mu \rightarrow \nu_\mu$ and $\bar{\nu}_\mu \rightarrow \bar{\nu}_\mu$.

The flux considered for set-up (a) has mean energy ~ 0.3 GeV, which are computed for 3.5 GeV protons and 10^{23} protons on target per year. For our analysis the beam power has been considered of about 4 MW per year and the time period has been taken to be 2 years for neutrinos and 4 years for anti-neutrinos. We consider the same flux as in [14, 82]. In the case of set-up(a) the efficiencies for the signal and background are included in the migration matrices based on [79] except for the channels ν_μ disappearance, $\bar{\nu}_\mu$ disappearance and ν_μ (NC) which are 64%, 81% and 11.7% efficiencies respectively. We have considered systematic uncertainties of 2% on signal and background channels.

The experimental set-up (b) has been considered as given in GLOBES [83] and the detector specification is mentioned in table III:

Target Power	4 Mega-Watt
Fiducial Mass	500 kt
Data Taking	4 yrs ν and 4 yrs $\bar{\nu}$
Baseline	295 km
Energy Resolution	0.085

TABLE III: Detector characteristics for Hyper-Kamiokande.

The flux considered for set-up (c) has mean energy ~ 5 GeV, which are computed for 50 GeV protons and 3×10^{21} protons on target per year. For our analysis the beam power is about 0.8 MW per year and the time period has been taken to be 5 years each for neutrinos and anti-neutrinos. We consider the same flux as in [18]. The detector characteristics for set-up (c) is given in table IV [84]. The correlation between the visible energy of background NC events and the neutrino energy is implemented by migration matrices which has been provided by L. Whitehead [85].

In table V for $\delta = 0$ we have shown the expected number of events for three experimental set-ups, for no NSIs and also for different real NSIs, each of which equal to α (one NSI at a time). We have considered the central values of various parameters as shown in table II and have used PREM profile [75] for matter densities. One can see that there is significant effect of $\varepsilon_{e\mu}$ and $\varepsilon_{e\tau}$ on the number of $\nu_\mu \rightarrow \nu_e$ events.

Signal Studies	ν_e CC appearance Studies	ν_μ CC Disappearance Studies
Signal efficiency	80%	85%
ν_μ NC mis-identification rate (Background)	1%	0.5%
ν_μ CC mis-identification rate (Background)	1%	0%
Signal Normalization error	5%	10%
Background Normalization Error	15%	20%
Neutrino Energy Resolution		
ν_e CC energy resolution	$0.15\sqrt{E(\text{GeV})}$	
ν_μ CC energy resolution	$0.2\sqrt{E(\text{GeV})}$	
E_{ν_μ} scale uncertainty	2%	
E_{ν_e} scale uncertainty	0.01%	

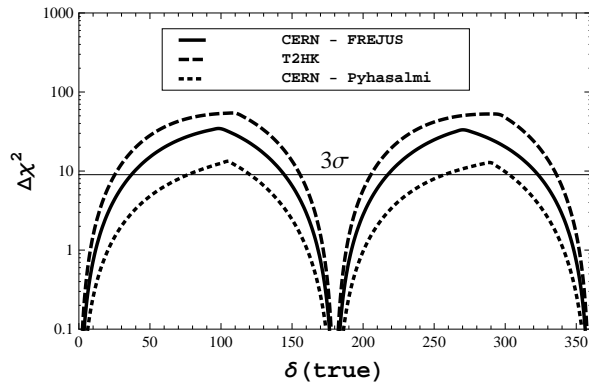
TABLE IV: Detector characteristics for set-up (c).

	CERN-Fréjus (130 km)	T2HK (295 km)	CERN-Pyhäsalmi (2300 km)
SM	4533	6098	421
ε_{ee}	4536	6110	426
$\varepsilon_{e\mu}$	4634	6272	502
$\varepsilon_{e\tau}$	4543	6143	470
$\varepsilon_{\mu\tau}$	4529	6081	414
$\varepsilon_{\mu\mu}$	4533	6099	425
$\varepsilon_{\tau\tau}$	4530	6085	413

TABLE V: The number of $\nu_\mu \rightarrow \nu_e$ events for CERN-Fréjus (130 km), T2HK (295 km) and CERN-Pyhäsalmi (2300 km) for SM and for different NSI (one at a time each of which equals to α).

Possibilities of significant effect of these NSIs can be seen in the expression of oscillation probabilities in Eq.(10).

2. Results

FIG. 1: Discovery reach of CP violation due to δ for three different experimental set-up : CERN-Fréjus, T2HK and CERN-Pyhäsalmi set-up considering only SM interactions for normal hierarchy.

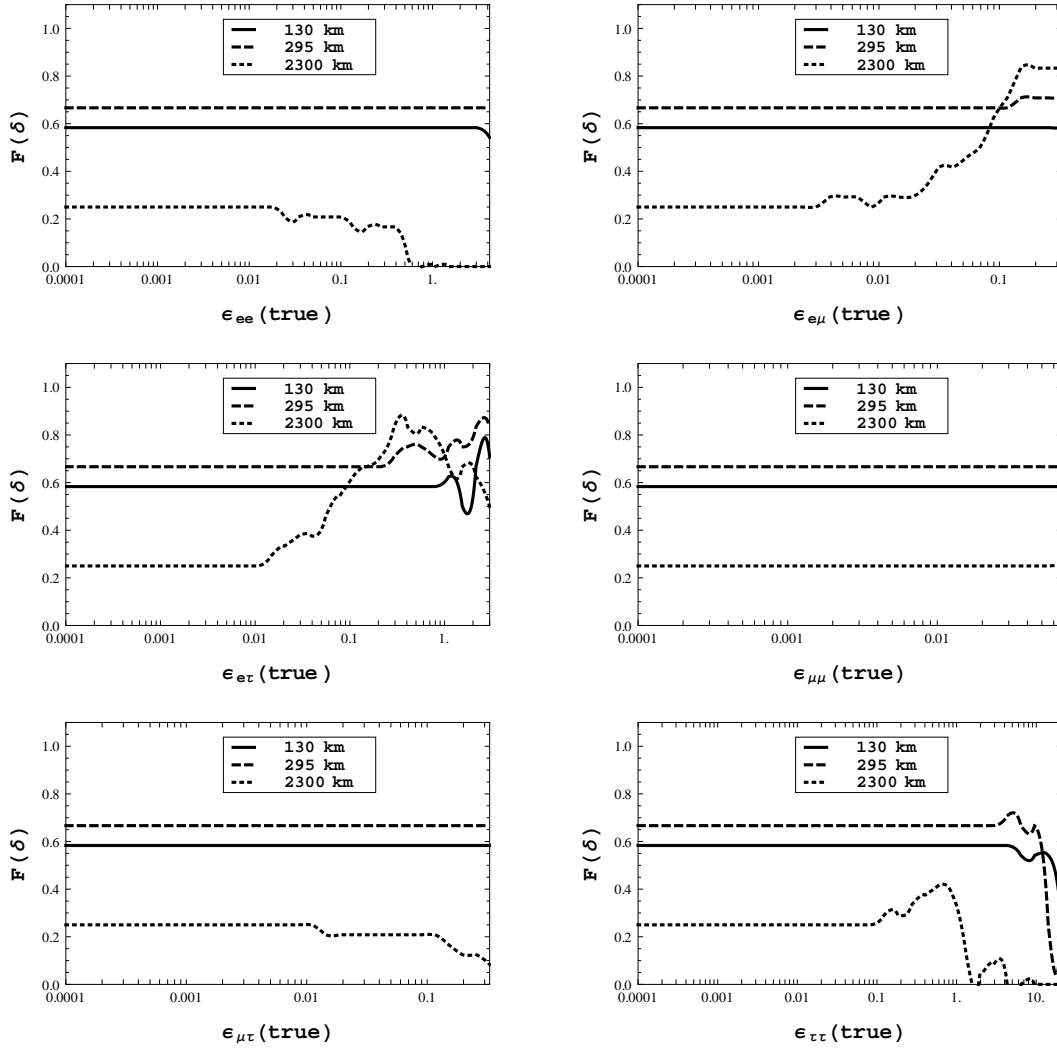


FIG. 2: $F(\delta)$ for three different experimental set-up: CERN-Fréjus, T2HK and CERN-Pyhäsalmi set-up at 3σ considering real NSIs ϵ_{ee} , $\epsilon_{e\mu}$, $\epsilon_{e\tau}$, $\epsilon_{\mu\mu}$, $\epsilon_{\mu\tau}$ and $\epsilon_{\tau\tau}$.

Here we first discuss the CP violation discovery reach without any NSI for the three experimental set-ups (a), (b) and (c). Then we make a comparative study between no NSI and with real NSI. We also consider off-diagonal NSIs with phases. The Figures are given only for normal hierarchy (true). However, there is no significant departures in the results for inverted hierarchy from that with normal hierarchy.

In Figure 1 we have shown the $\Delta\chi^2$ values versus $\delta(\text{true})$ for SM interactions of neutrinos with matter from which the discovery reach can be obtained at different confidence levels. We have fixed $\delta(\text{test})$ to 0 and π and have marginalized over hierarchy for every $\delta(\text{true})$ value. To calculate CP fraction from Figure 1 at 3σ one is required to find the fraction of the total allowed range of δ for which $\Delta\chi^2$ values are above the solid horizontal line in Figure 1. Particularly at 3σ confidence level for CERN-Fréjus set-up the CP violation could be discovered with $F(\delta)$ of around 0.58 of the possible δ values for normal hierarchy (true value) whereas for T2HK set-up these values are around 0.67 and for CERN-Pyhäsalmi set-up these values

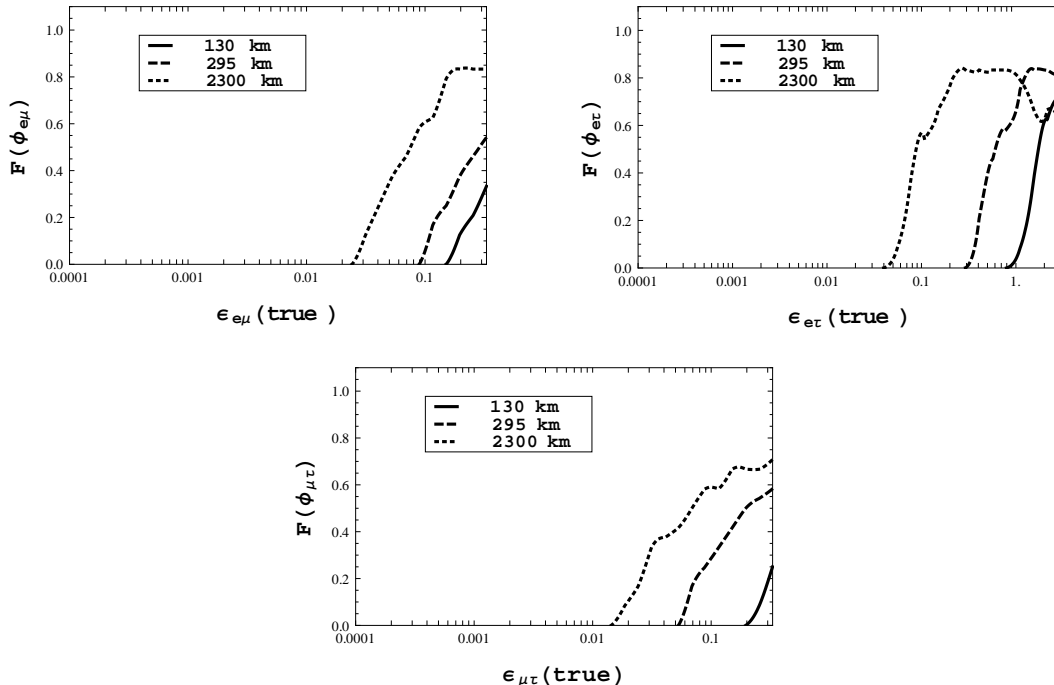


FIG. 3: $F(\phi_{e\mu})$, $F(\phi_{e\tau})$ and $F(\phi_{\mu\tau})$ (one NSI at a time) for $\delta_{CP} = 0$ at 3σ confidence level for three different experimental set-up.

are about 0.21. For longer baseline for normal hierarchy the discovery reach is little bit better than the inverted hierarchy (not shown in the Figure). The discovery reach for longer baseline of 2300 km was shown earlier by Coloma *et al* [18]. So with only SM interactions of neutrinos with matter the short baseline like T2HK set-up seems to be better for good discovery reach of CP violation. This was observed earlier by different authors [18, 19, 24–26].

a. Possibilities of Discovery of CP violation due to δ for real NSI: If we compare the $F(\delta)$ obtained from Figure 1 at 3σ with that shown in Figure 2 at 3σ we find that for smaller values of NSIs satisfying model dependent bound for short baseline of CERN-Fréjus and T2HK set-up, there is insignificant effect of NSI on the the discovery reach of CP violation due to δ . However, for CERN-Pyhäsalmi set-up even for smaller NSI values one finds the effect on CP violation discovery reach. One interesting feature is found from these figures which is that if one does not observe CP violation due to δ in shorter baselines (say CERN-Fréjus set-up) there is still a possibility of observing CP violation in longer baselines (see CERN-Pyhäsalmi set-up with off-diagonal NSI like $\varepsilon_{e\mu}$ and $\varepsilon_{e\tau}$) which could be the signal of NSI with significant strength. In Figure 2 one can see that except $\varepsilon_{\mu\mu}$ for other NSIs the $F(\delta)$ changes considerably, with increase in the values of different NSIs for CERN-Pyhäsalmi set-up.

b. Possibilities of Discovery of CP violation due to complex NSI phases : There could be CP violation only due to off-diagonal NSI phases for which $\delta = 0$. Such cases have been shown in Figures 3. We observe that for certain NSI value the CP fraction for longer baselines is more in comparison to that for the shorter baselines. With the increase of $|\varepsilon_{\alpha\beta}|$ there is increase in discovery of CP fraction in general. If CP violation is not observed in short baselines (say CERN-Fréjus) but it is observed at relatively longer

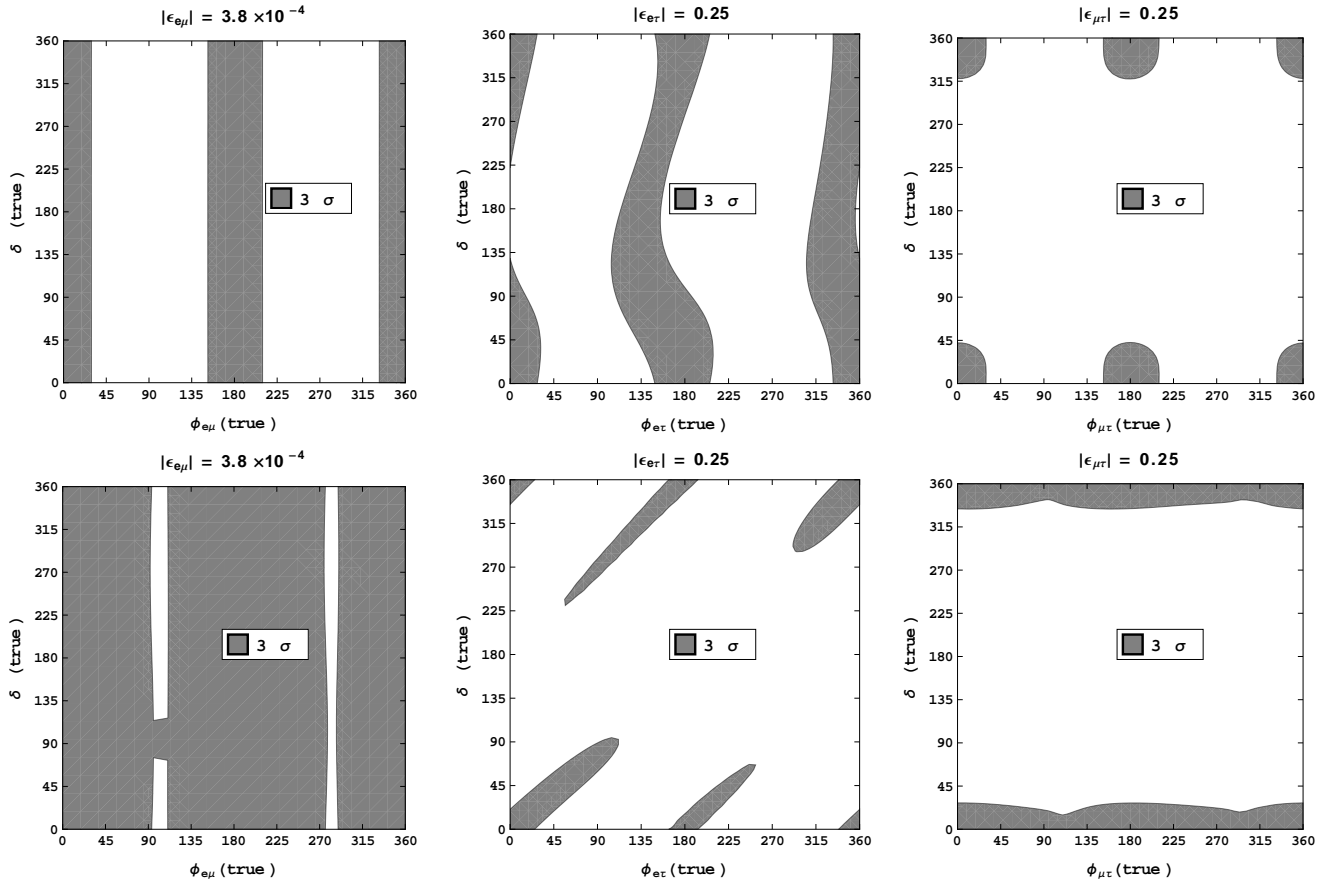


FIG. 4: Allowed region (unshaded) for total CP violation discovery reach $F(\delta)$ for two different baselines T2HK (top panel) and CERN-Pyhäsalmi set-up (bottom panel) considering NSI phases $\phi_{e\mu}$, $\phi_{e\tau}$ and $\phi_{\mu\tau}$.

baselines (say CERN-Pyhäsalmi set-up) then it would signal the presence of NSI as can be seen from Figure 3.

c. Possibilities of Discovery of CP violation due to both δ and complex NSI phases : In Figure 4 in the un-shaded region discovery of total CP violation could be possible at 3σ confidence level. Here, we are assuming that nature has two sources of CP violation - one due to δ phase and other due to one NSI phase. For this we ask whether there is $(\delta - \phi_{ij})$ parameter space where both can be distinguishable from their CP conserving points as discussed earlier. From the Figure it is seen that for T2HK set-up there is more allowed region and as such better discovery reach in the $\delta - \phi_{ij}$ parameter space particularly for NSI - $\varepsilon_{e\mu}$ in comparison to CERN-Pyhäsalmi set-up . Particularly for NSI - $\varepsilon_{e\tau}$ and $\varepsilon_{\mu\tau}$, the discovery reach of total CP violation is better for both longer and shorter baselines (like CERN-Pyhäsalmi set-up and T2HK set-up). Simultaneous consideration of experimental data from both these set-ups could improve the discovery reach further because of presence of non-overlapping un-shaded discovery regions in the upper panel two right Figures and lower panel two right Figures corresponding to two different NSIs.

From Figure 1 it is observed that for certain range of values of δ (about 0° to 25° , 160° to 208° , 340° to 360°), the CP violation due to δ could remain unobservable. However, even if nature has such values of δ , from

Figure 4 one can see that total CP violation could be observed in such cases in presence of NSI for a wide range of values of different NSI phases. However, disentangling the sources of two types of CP violating phases (one from NSI phase and other from δ) could be difficult. Here the total CP fraction can be thought of as the ratio of the un-shaded region divided by the total region covered by $\delta - \phi_{ij}$ parameter space. As for example, in the upper panel extreme left Figure such total CP fraction is about 75%. For both the set-ups for $\varepsilon_{e\tau}$ such CP fraction is even more. For CERN-Pyhäsalmi set-up for $\varepsilon_{e\mu}$ the total CP fraction is not good.

B. Neutrino factory

We discuss below the experimental set-up and systematic errors for neutrino factory. We have presented our results for discovery reach of CP violation for different baselines of length 730 km (FNAL-Soudan), 1290 km (FNAL-Homestake) and 1500 km (FNAL-Henderson) due to δ and other off-diagonal NSI phases ϕ_{ij} . We have shown the effect of the absolute values of different $\varepsilon_{\alpha\beta}$ in that. For this analysis we have considered one NSI at a time.

1. Experimental set-ups and systematic errors

We have used a large magnetised iron neutrino detector(MIND) [44] with a toroidal magnetic field having a mass of 100 KTon. MIND can also be described as an iron-scintillator calorimeter. This detector has the capability of excellent reconstruction and charge detection efficiency. In this section we have considered muons in a storage ring consisting of both μ^+ and μ^- which decay with energies of 10 GeV. We consider 5×10^{21} stored muons. The golden channel ($\nu_e \rightarrow \nu_\mu$ oscillation channel) where the charged current interactions of the ν_μ produce muons of the opposite charge to those stored in the storage ring (generally known as wrong-sign muons), is the most promising channel to explore CP violation at a neutrino factory. The detector that we are considering in this work - MIND is optimized to exploit the golden channel oscillation as this detector has the capacity to easily identify signal i.e. a muon with a sign opposite to that in the muon storage ring. Different oscillation channels which have been considered as signals and backgrounds [44] in the analysis are shown in table VI. We have taken the migration matrices for the true and reconstructed neutrino energies as given in reference [44]. The signal and background efficiencies are taken into account in those matrices. We have taken into account the reconstruction of τ contamination coming from the *silver channel* $\nu_e \rightarrow \nu_\tau$ as background. We have considered systematic errors to be 1%. In this work we have considered a running time of 5 years for both μ^+ and μ^- .

	Channel Name	μ^+	μ^-
Signal	Golden Channel	$\nu_e \rightarrow \nu_\mu$	$\bar{\nu}_e \rightarrow \bar{\nu}_\mu$
Background	ν_e disappearance channel	$\nu_\mu \rightarrow \nu_e$	$\bar{\nu}_\mu \rightarrow \bar{\nu}_e$
	Silver Channel	$\nu_e \rightarrow \nu_\tau$	$\bar{\nu}_e \rightarrow \bar{\nu}_\tau$
	ν_μ disappearance channel	$\bar{\nu}_\mu \rightarrow \bar{\nu}_\mu$	$\nu_\mu \rightarrow \nu_\mu$
	Platinum Channel	$\bar{\nu}_\mu \rightarrow \bar{\nu}_e$	$\nu_\mu \rightarrow \nu_e$
	Dominant Channel	$\bar{\nu}_\mu \rightarrow \bar{\nu}_\tau$	$\nu_\mu \rightarrow \nu_\tau$

TABLE VI: Different oscillation channels considered as signals and backgrounds in the analysis.

	730 km	1290 km	1500 km
SM	248491	222097	210819
ε_{ee}	248715	222644	211527
$\varepsilon_{e\mu}$	316049	283709	269412
$\varepsilon_{e\tau}$	251331	229148	220134
$\varepsilon_{\mu\tau}$	248049	220985	209394
$\varepsilon_{\mu\mu}$	248682	222667	211597
$\varepsilon_{\tau\tau}$	248072	220964	209313

TABLE VII: Number of $\nu_e \rightarrow \nu_\mu$ events for 730 km (FNAL-Soudan), 1290 km (FNAL-Homestake) and 1500 km (FNAL-Henderson) for SM and for different NSI (one at a time each of which equals to α).

In table VII for $\delta = 0$ we have shown the expected number of events for three baselines in neutrino factory, for no NSI and also for different real NSI, each of which equal to α (one NSI at a time). We have considered the central values of various parameters as shown in table II and have used PREM profile [75] for matter densities. Like superbeam case here also for neutrino factory one can see that there is significant effect of $\varepsilon_{e\mu}$ and $\varepsilon_{e\tau}$ on the number of $\nu_e \rightarrow \nu_\mu$ events. Possibilities of significant effect of these NSIs can be seen in the expression of oscillation probabilities $\nu_e \rightarrow \nu_\mu$ (which can be obtained using Eq.(13) in Eq.(10)).

2. Results

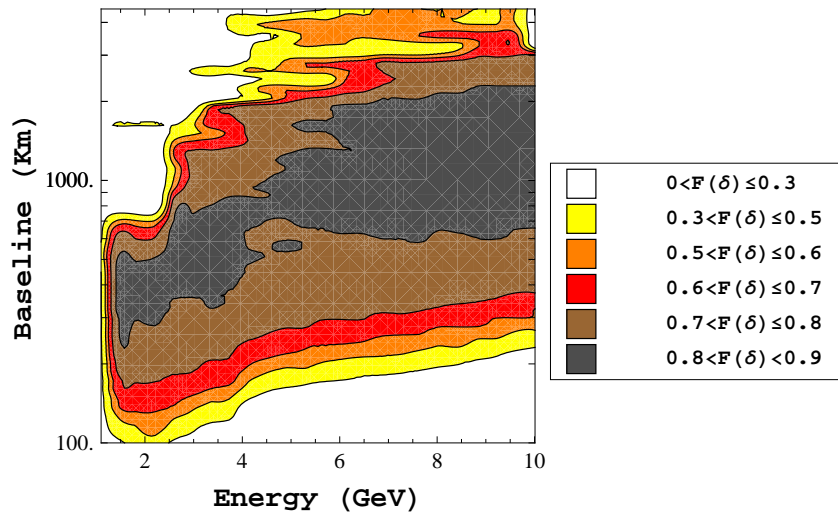


FIG. 5: $F(\delta)$ with only SM interactions of neutrinos with matter for baselines of different lengths and different muon energies E_μ at 5σ confidence level.

The optimization of CP violation discovery reach has been done earlier [29, 30] for different baselines and different parent muon energy when only SM interactions of neutrinos with matter during propagation is present. We have re-analysed this optimization based on the updated MIND detector characteristics and the migration matrices as given in [44]. We present the result for neutrino factory at 5σ confidence level unlike

superbeam case where we have given the results at 3σ confidence level. This is because MIND detector for neutrino factory is found to give quite good CP violation discovery reach. It is found that at 5σ confidence level the CP fraction (shown as $F(\delta)$ in Figure 5) of about ($0.8 \leq F(\delta) < 0.9$) is possible for baselines ranging from about 300 to 800 km for energies lesser than 5 GeV and for baselines ranging from about 700 to 2000 km for energies 6-10 GeV respectively. Based on high CP fraction discovery potential as found in this Figure we have chosen 10 GeV muon energy and a few baselines which are : 730 km(FNAL-Soudan), 1290 km (FNAL-Homestake) and 1500 km (FNAL-Henderson).

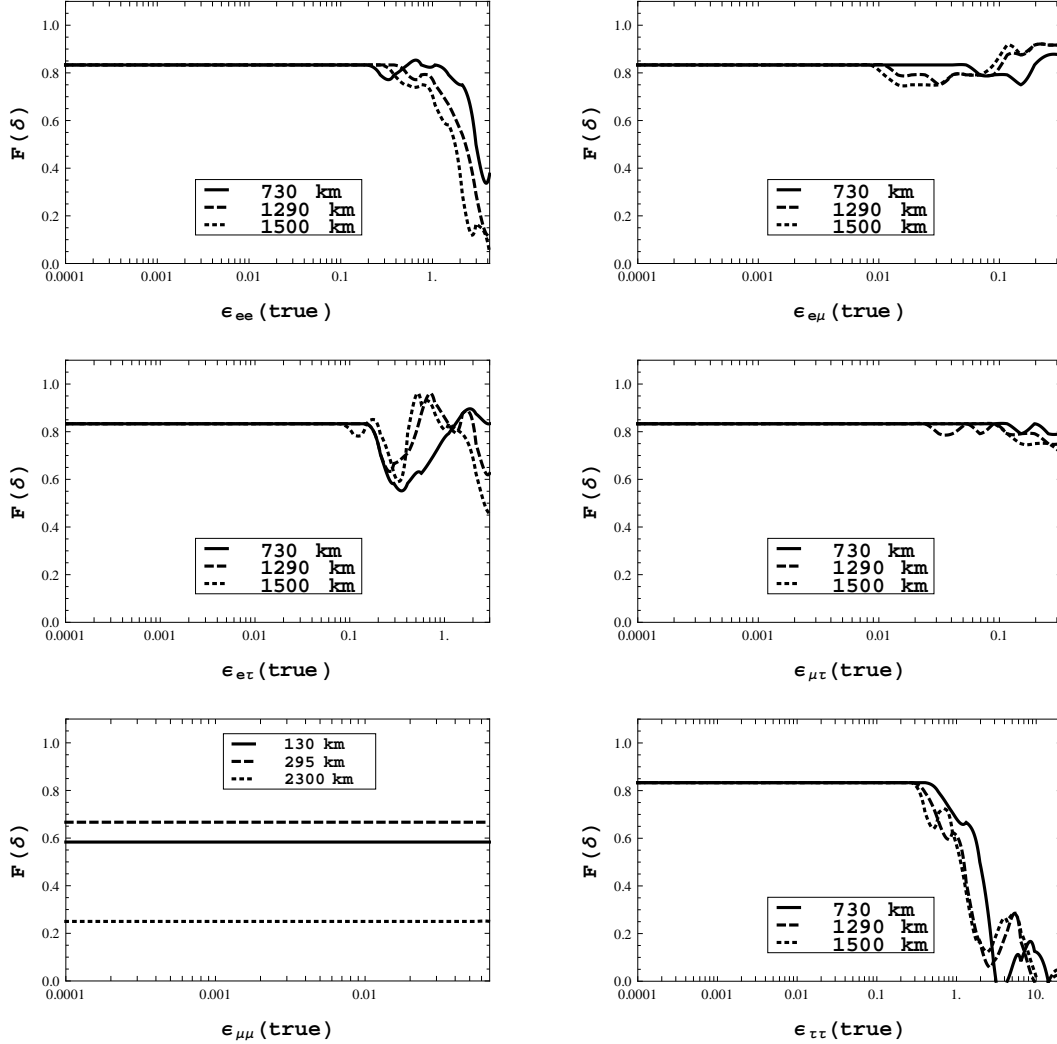


FIG. 6: $F(\delta)$ versus real NSI (ϵ_{ij}) at 5σ confidence levels.

Next we have tried to answer the question that had there been non-Standard interactions what could have been their effect on the CP violation discovery reach for such experimental set-ups. While taking into account NSI effect, for off-diagonal NSI we have also considered the effect of NSI phases over δ_{CP} violation. In contrast to the results on superbeam we have presented results for neutrino factory at 5σ confidence level in Figures 6 and 7 because in most of the cases the discovery reach of CP violation is far better in neutrino

factory set-ups than those in superbeam set-ups particularly for NSIs $\lesssim 1$. However, for comparison of the results of neutrino factory set-ups with that of superbeam set-ups we have considered the 3σ results for both type of set-ups. For brevity we have avoided presenting the results at 3σ corresponding to Figures 6 and 7.

a. Possibilities of Discovery of CP violation due to δ for real NSI: In Figure 6, we have studied $F(\delta)$ in the presence of real NSI (NSI phases have been chosen to be zero) for different baselines of length 730 km, 1290 km and 1500 km at 5σ confidence level. Here, in plotting the Figures we have considered the NSI values upto the model independent bounds as shown in table I. For lower values of NSI there is essentially negligible effect on discovery reach of CP violation which is seen in the Figure as horizontal straight line. This corresponds to $F(\delta)$ due to SM interactions only which can be verified from Figure 5 at muon energy of 10 GeV for the appropriate baseline. For NSI $\varepsilon_{\mu\mu}$ with model dependent bound there is insignificant effect on $F(\delta)$ whereas for other NSIs there are some effect on $F(\delta)$. Except $\varepsilon_{e\mu}$, $\varepsilon_{e\tau}$ and $\varepsilon_{\mu\mu}$ for other NSIs there is considerable decrease in discovery reach of CP violation with the increase of NSI values. Even if there is CP violating phase δ but as one can see that in presence of higher allowed values of NSI - $\varepsilon_{\tau\tau}$ there could be no discovery of δ_{CP} violation.

The results are shown in Figure 6 at 5σ confidence level. However, at 3σ also the decreasing features of ε_{ee} and $\varepsilon_{\tau\tau} \gtrsim 1$ is present and in comparison to Figure 2 it is found that for large NSI values of $\varepsilon_{ee}, \varepsilon_{\tau\tau} \gtrsim 1$ superbeam T2HK set-up is found to be better for the discovery reach of CP violation as compared to neutrino factory set-ups. But for lower values of NSIs particularly $\varepsilon \lesssim 10^{-1}$ the neutrino factory set-ups are found to be much better for the discovery of CP violation at 3σ and even at 5σ the CP fraction is more in neutrino factory set-ups.

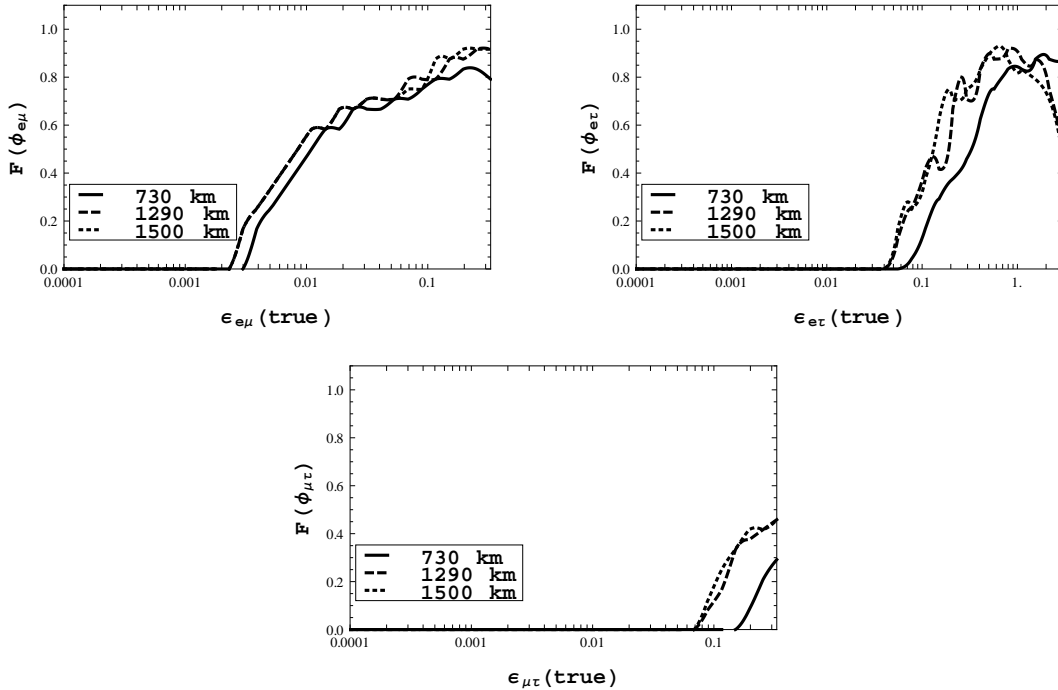


FIG. 7: $F(\phi_{e\mu})$, $F(\phi_{e\tau})$ and $F(\phi_{\mu\tau})$ for $\delta_{CP} = 0$ at 5σ confidence level for three baselines.

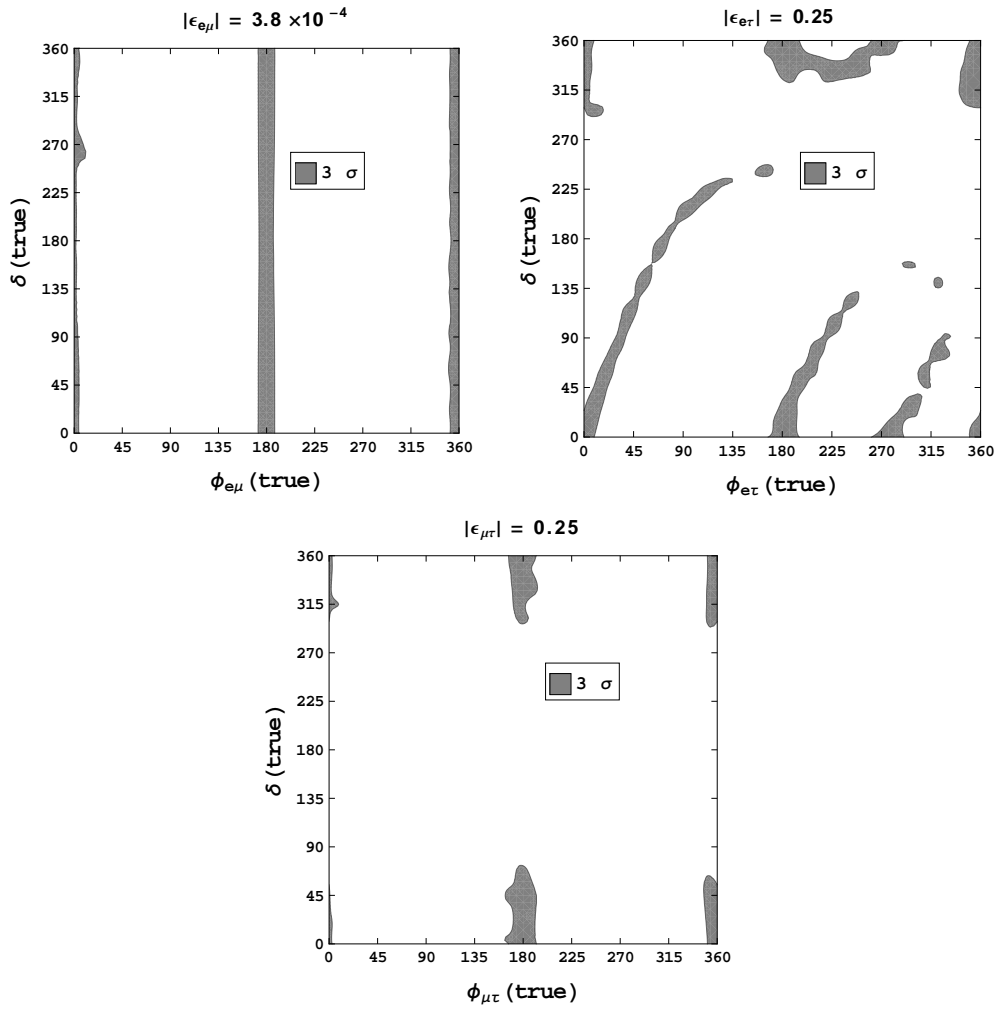


FIG. 8: δ versus phase (ϕ_{ij}) considering the value of NSIs(ϵ_{ij}) at the uppermost value with model dependent bounds. Unshaded regions correspond to CP violation discovery reach.

b. Possibilities of Discovery of CP violation due to complex NSI phases : In Figure 7 we have addressed the question of what could be the CP fraction for discovery of CP violation if Dirac phase δ is absent in PMNS mixing matrix and CP violation comes from purely NSI phases. We observe that for certain NSI value the CP fraction for longer baselines could be more in comparison to that for the shorter baselines. With the increase of $|\epsilon_{\alpha\beta}|$ there is increase in discovery of CP fraction in general. If CP violation is not observed in short baselines (say 730 km) but it is observed at relatively longer baselines (say 1500 km) then it would signal the presence of NSI as can be seen from our Figures although for $\epsilon_{e\mu}$ it is difficult to distinguish the effect between short and long baselines considered by us. Comparing 3σ result of neutrino factory (not shown here) with superbeam result of Figure 3 it is found that in the presence of $\epsilon_{e\mu}$ the Neutrino factory set-up gives better CP violation discovery reach whereas for $\epsilon_{\mu\tau}$ the superbeam CERN-Pyhäsalmi set-up is better. For $\epsilon_{e\tau}$ the neutrino factory set-up is slightly better than superbeam set-up.

c. Possibilities of Discovery of CP violation due to both δ and complex NSI phases : In Figures 8 we have considered the case for 730 km baseline where the CP violation might come from δ_{CP} as well as from NSI phase $\phi_{\alpha\beta}$. For 1290 km and 1500 km baselines the essential feature is almost same (not shown in the Figure). Here we have chosen the uppermost value of NSI with model dependent bound. The total CP violation due to δ and ϕ_{ij} could be observable even for those δ which could remain unobservable in absence of NSI phases for some ranges of δ values. In fact, the CP violation discovery reach could be possible for the whole range of allowed δ values for some specific values of ϕ_{ij} as can be seen from Figures. But it would be difficult to conclude whether the observed CP violation is due to δ or any NSI phase. As compared to Figure 4 due to different superbeam set-ups, we find better discovery reach of CP violation for neutrino factory set-up for 730 km baseline in Figures 8. As for example, in the extreme left Figure for $\varepsilon_{e\mu}$ the total CP fraction is around 94% for neutrino factory in contrast to 75% for the T2HK superbeam set-up as shown in Figures 4.

Comparing Figures 8 and 4 we find that for $\phi_{e\tau}$ if we combine experimental data from superbeam set-ups and neutrino factory set-ups, there are scopes to improve the total CP violation discovery reach further.

C. monoenergetic neutrino beam

We discuss below the possible discovery reach of CP violation for two different nuclei, ^{110}Sn and ^{152}Yb which is considered for the electron capture experiment. We also discuss our procedure of energy resolution at the detector for numerical simulation. Earlier in section II we have shown how $\nu_e \rightarrow \nu_\mu$ oscillation probability depends on δ for shorter baseline ($A \sim \alpha$). Based on the oscillation probability and its' variation with respect to δ we discuss the procedure for choosing suitable boost factor γ numerically for specific baseline and specific nuclei considered for the neutrino beam. We mention below four experimental set-ups that we have considered for analysis of discovery reach of CP violation with monoenergetic neutrino beam.

1. Suitable boost factor, neutrino energy from $\nu_e \rightarrow \nu_\mu$ oscillation probability

The most suitable candidate for producing neutrino beam from electron capture process would be the one with a low Q value and high boost factor, γ [48]. Also it would be preferable if the nuclei has a short half life. The reason for these is as follows. We need neutrino energy around the peak of the oscillation probability where variation due to δ is significant and as such $\frac{\Delta m_{31}^2 L}{4E} \approx (2n + 1)\frac{\pi}{2}$. Considering $E = 2\gamma Q$, it follows that $\gamma = \frac{\Delta m_{31}^2 L}{4\pi Q}$ as for example, for the first oscillation peak. For sufficiently high γ almost all neutrinos are expected to go through the detector. Then to satisfy the above condition we need to lower Q value. Then another condition is, $\gamma\tau < T$ where T is the time considered to perform the experiment so that all the nuclei decay and τ is the half life of the nuclei. If γ is increased then the half life τ is required to be small. So the preferable factors considered in choosing the candidate for producing neutrino beam from electron capture process are - low Q value, small half life τ and high γ [48]. Although higher γ needs technological advancement for the accelerator.

The isotope, ^{110}Sn , has $Q = 267$ keV in the rest frame and a half life of 4.11 h. As it has a low Q value so one may consider high γ value. However, it has a longer half life as compared to other nuclei like ^{150}Er , ^{152}Yb , ^{156}Yb , ^{150}Dy , ^{148}Dy [47, 50] whose half lifes are 18.5 seconds, 3.04 seconds, 261 seconds, 7.2 min and

3.1 min respectively. However, these nuclei have larger Q values of the order of 10^3 keV. On the other hand, considering effective running time per year as 10^7 second all the nuclei for isotope $^{110}_{50}\text{Sn}$ will not decay. But for $\gamma = 500$ or 320 (as considered in our analysis to obtain the suitable neutrino energy E resulting in high oscillation probability) the useful decays are respectively about 0.608 or 0.768 times the total number of $^{110}_{50}\text{Sn}$ nuclei considered. So there is not much suppression in numbers of nuclei. Hence although $^{110}_{50}\text{Sn}$ has a larger half life, due to its lower Q value there is scope to consider higher γ for CERN-Fréjus or 250 km baselines. For these reasons we have preferred isotope, $^{110}_{50}\text{Sn}$ in comparison to other nuclei. However, there is recent study on finding suitable candidate nuclei for electron capture process and it has been found that ^{150}Er , ^{152}Yb , ^{156}Yb nuclei have dominant electron capture decay to one level. Particularly, ^{152}Yb has been found to be most suitable one [50]. For this reason, apart from nuclei $^{110}_{50}\text{Sn}$ we shall consider ^{152}Yb also for our analysis. However, as Q value (5435 keV) for ^{152}Yb is higher, corresponding γ value for such nuclei are supposed to be small.

The neutrino beam produced from electron capture process is boosted with certain boost factor, γ . The boosted neutrino beam produced from such process hits the detector at a baseline of length L at a radial distance R from the beam axis and the energy, E of this beam in rest frame of the detector, i.e., in laboratory frame is given by:

$$E(R) = \frac{Q}{\gamma} \left[1 - \frac{\beta}{\sqrt{1 + (R/L)^2}} \right]^{-1} \approx \frac{2\gamma Q}{1 + (\gamma R/L)^2} \quad (22)$$

where R is the radial distance at the detector from the beam axis. At beam center, $R = 0$. From the above equation (22) the energy window considered for the analysis which is constrained by the size of the detector is given by:

$$\frac{2\gamma Q}{1 + (\gamma R_{max}/L)^2} \leq E \leq 2\gamma Q \quad (23)$$

From equation (23) we can see that once the baseline length L and γ is fixed the energy window gets fixed. However, even considering radius of the detector $R_{max} = 100$ m the energy window is very small as can be seen from Figure 9.

One can see from equation Eq.(22) that it is possible to tell precisely the energy from the R value of the Cherenkov ring at the Cherenkov detector instead of measuring directly the neutrino energy. So there is scope to get good energy resolution by measuring position if the vertex resolution is good. The $\sigma(E)$ function corresponding to energy resolution function (as used in running GLOBES [76]) in terms of vertex measurement uncertainty $\sigma(R)$ can be written as:

$$\sigma(E) = - \frac{QR\beta}{L^2 \left(1 + \frac{R^2}{L^2}\right)^{3/2} \left(1 - \frac{\beta}{\sqrt{1 + \frac{R^2}{L^2}}}\right)^2} \sigma(R) \quad (24)$$

where β is defined as

$$\beta = \frac{\sqrt{\gamma^2 - 1}}{\gamma} \quad (25)$$

Vertex measurement uncertainty for electron (muon) identification at Super-K is around 30 (20) cm [86]. To estimate the energy resolution using position measurement one may consider $\sigma(R) \sim 30$ cm provided that the beam spreading $\frac{\sigma(R)}{L}$ is negligible (lesser than about $1\mu\text{rad}$) [45] which is difficult to achieve experimentally. If we take into account the beam divergence about $10\mu\text{rad}$ (which is almost one order larger than that considered in references [87, 88]), one may consider larger $\sigma(R) \sim 130$ cm particularly for baseline of 130 km. For baseline like 250 km it would be more but we have considered same $\sigma(R)$ which means the beam divergence has been assumed to be lesser than about $5\mu\text{rad}$ for the analysis for baseline with length 250 km.

In this work GLoBES[76] has been used for doing the simulations. In order to use this software, the radial binning is replaced by binning in energy and the bins are not equidistant. If we divide R_{max}^2 into k bins the edges of the bins are given as:

$$R_i^2 = R_{max}^2 - (i - 1)\Delta R^2 \quad (26)$$

with

$$\Delta R^2 = \frac{R_{max}^2}{k} \quad (27)$$

We consider $R_i^2 > R_{i+1}^2$ so that in GLoBES the respective energy bins are in the correct order as given below

$$E(R_i^2) < E(R_{i+1}^2) \quad (28)$$

where E is the neutrino energy in the lab frame.

The number of events per bin i and channel c (different channels mentioned later in this section) is given by:

$$N_{event} \simeq \frac{N_{norm}}{L^2} \int_{E_i - \Delta E_i/2}^{E_i + \Delta E_i/2} dE' \int_0^\infty dE \phi(E) P^c(L, E) \sigma^c(E) \epsilon^c(E') R^c(E, E') \quad (29)$$

where N_{norm} is the normalization factor for using GLoBES and is related to length of the baseline, area and energy binning related to flux, number of target nuclei per unit target mass and number of nuclei decaying. ϵ^c is the signal efficiency in the respective channel, $P^c(L, E)$ is the neutrino oscillation probability in particular channel, $\sigma^c(E)$ is total cross section for particular flavor of neutrinos and particular interaction corresponding to particular channel. $R(E, E')$ is the energy resolution function of the detector where E' is the reconstructed neutrino energy. $\phi(E)$ has been calculated from the angular neutrino flux $\frac{dn}{d\Omega}(E)$ as

defined below :

$$\frac{dn}{d\Omega} = \frac{N_{decays}}{4\pi} \left(\frac{E}{Q}\right)^2 \quad (30)$$

where N_{decays} is number of nuclei actually decaying per year. The detailed derivation of these expressions can be found in [45]. Considering equation (23) and (30) one can see that with increase in γ value the angular flux increases.

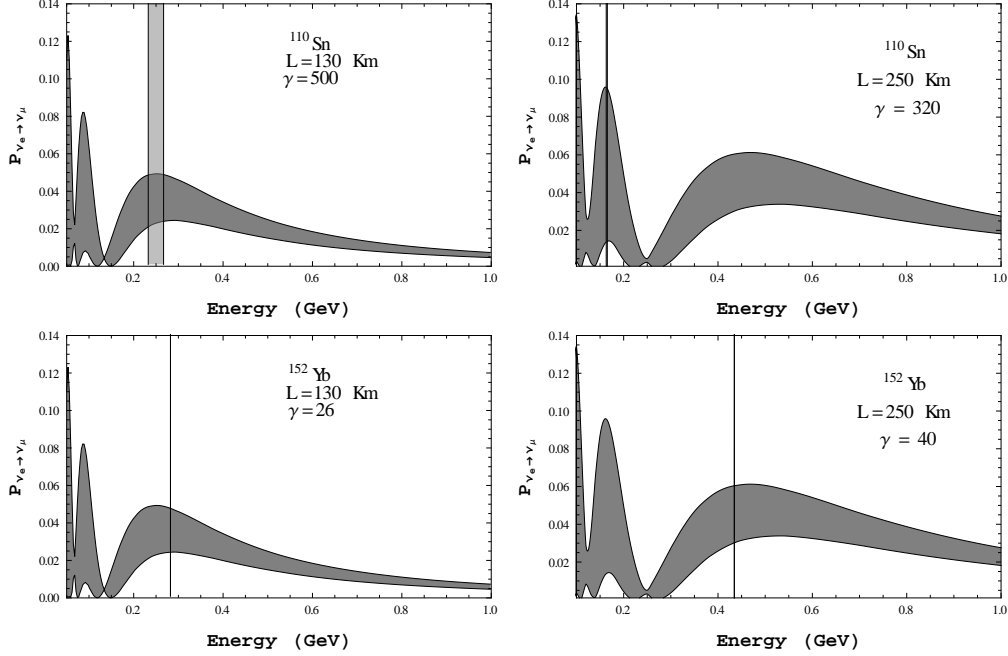


FIG. 9: Probability $P(\nu_e \rightarrow \nu_\mu)$ vs neutrino energy E for two different nuclei $^{110}_{50}\text{Sn}$ and $^{152}_{70}\text{Yb}$ and the corresponding energy window satisfying equation (23) for different γ values.

We have plotted numerically the probability $P(\nu_e \rightarrow \nu_\mu)$ with respect to energy for two different baselines of length 130 km (CERN-Fréjus) and 250 km for two different nuclei $^{110}_{50}\text{Sn}$ and $^{152}_{70}\text{Yb}$. We have considered normal hierarchy in plotting Figure 9. For all plots in Figure 9, δ has been varied over its' entire allowed range (0 to 2π) resulting in the shaded region in each plots showing the significant variation of probability at particular neutrino energies. Corresponding to each of the nuclei (whose Q values are fixed) we have considered appropriate γ value so that the corresponding energy window (as mentioned in (23)) overlaps with the shaded region near the oscillation peaks having significant variation of probability due to δ variation. In choosing γ , one also has to keep in mind that the neutrino energy is not too low as otherwise flux will be much lesser. The energy window has been shown by the shaded vertical strips. For our suitable choice of γ value, the energy window is larger for 130 km baseline and relatively smaller for 250 km baseline for both the nuclei. Also the energy window for $^{110}_{50}\text{Sn}$ is larger than $^{152}_{70}\text{Yb}$.

For finding δ we shall prefer the maximum variation of the probability with δ which will occur for neutrino energy satisfying $\frac{\Delta m_{31}^2 L}{4E} \approx (2n + 1)\pi/2$ where n is an integer. This has been shown in Figure 9 in which

the oscillation probability has been evaluated numerically considering the evolution of neutrino flavor states. However, the energy also depends on the Q value of the corresponding nuclei. So we have considered the case of two nuclei separately. As for example, for $^{110}_{50}\text{Sn}$ nuclei, for baseline of length 130 km we have considered first oscillation maximum and for baseline of length 250 km we have considered second oscillation maximum where the variation of the probability due to δ is significant. For ^{152}Yb , for both the baselines we have considered first oscillation peak. In considering the suitable peak in the oscillation probability one has to keep in mind that the neutrino flux increases with E^2 as shown in Eq.(30) and so after doing the numerical analysis one can decide which energy out of various energies near various peaks are suitable. However, one also have to think about feasible boost factor γ . For that reason although the first oscillation peak for $^{110}_{50}\text{Sn}$ nuclei corresponds to higher energy with respect to 2nd oscillation peak but as it also requires higher boost factor γ around 900, we have considered the neutrino energy near the second oscillation peak for $^{110}_{50}\text{Sn}$ nuclei for baseline of length 250 km. Depending on the energy chosen near a peak one can appropriately choose the boost factor γ on which the neutrino energy window as shown in equation (23) as well as ν_e flux as shown in equation (30) depend. This has been illustrated in Figure 9.

2. Experimental set-ups and systematic errors

For doing the analysis we choose four different set-ups:

set-up(a): The length of the baseline is taken to be 130 km (CERN-Fréjus baseline) and the boost factor γ to be 500 for nuclei $^{110}_{50}\text{Sn}$.

set-up(b): The length of the baseline is taken to be 250 km and the boost factor γ to be 320 for nuclei $^{110}_{50}\text{Sn}$.

set-up(c): The length of the baseline is taken to be 130 km (CERN-Fréjus baseline) and the boost factor γ to be 26 for nuclei ^{152}Yb .

set-up(d): The length of the baseline is taken to be 250 km and the boost factor γ to be 40 for nuclei ^{152}Yb .

We consider a Water Cherenkov detector of fiducial mass 500 kt. Following [89], the signal efficiency is considered to be 0.55 for ν_μ appearance channel. Background rejection factor coming from neutral current events is considered to be 10^{-4} for ν_μ appearance channel. Signal error of 2.5% and background error of 5% has been considered. For quasi-elastic ν_μ appearance and ν_e disappearance we have followed signal efficiency and error as given in reference [89]. We have considered the neutrino energy resolution as discussed earlier in (24) which can be obtained from vertex resolution after taking into account beam spreading. The neutrino energy is known from Eq.(22) and the energy width considered by us is obtained from Eq.(23) by considering the radius of the detector $R_{max} = 100\text{m}$. We assume 10^{18} electron capture decays per year and the running time of 10 years for accumulating data.

However, depending on the half life of Sn (4.11 hrs), the number of useful decays per effective year (10^7 seconds) considered are about 0.608×10^{18} with boost factor ($\gamma = 500$) for 130 km baseline and 0.768×10^{18} with boost factor ($\gamma = 320$) for 250 km baseline. Also, depending on the half life of ^{152}Yb (3.04 seconds) and the boost factor $\gamma = 26$ or $\gamma = 40$, for baselines 130 km or 250 km respectively, the number of useful decays per effective year (10^7 seconds) considered are almost equal to the total number of nuclei i.e, 10^{18} as half life is much smaller than $^{110}_{50}\text{Sn}$. It is possible to achieve γ about 480 at upgraded SPS facility at CERN [90–92] and $\gamma > 1000$ for LHC based design [93]. We have considered six energy bins keeping in mind the available energy window for different set-ups and the corresponding energy resolution in equation (24).

In considering the energy resolution we have taken into account beam spreading. For that the the energy resolution considered by us is bad in comparison to the energy resolution considered in reference [45] and we have to consider much lesser number of energy bins.

As the number of events corresponding to all set-ups are quite large, any background due to atmospheric neutrinos are expected to be quite small and we have not considered such background in our analysis.

3. Possibilities of Discovery of CP violation

Here we discuss the discovery of CP violation for four different experimental set-ups (a-d) mentioned earlier for monoenergetic neutrino beam. In presenting our analysis we have followed the numerical procedure as discussed at the beginning of section III. We have considered the true hierarchy as normal hierarchy. However, we have considered the uncertainty in the hierarchy of neutrino masses in the test values as it is not known at present. We have also considered the uncertainties in the other oscillation parameters as mentioned in table II. For finding CP violation we have fixed $\delta(\text{test})$ at CP conserving δ values $(0, \pi)$.

In Figure 10, $\Delta\chi^2$ versus δ (true) has been plotted to show the discovery reach of the CP violation for two different set-ups - set-up(a) and set-up(b) for ^{110}Sn nuclei. We find that the discovery of CP violation for set-up(a) & (b) could be found with $F(\delta)$ for about 51% and 49% respectively of the possible δ values at 3σ confidence level. In Figure 11, $\Delta\chi^2$ versus δ (true) has been plotted to show the discovery reach of the CP violation for two different set-ups - set-up(c) and set-up(d) for ^{152}Yb nuclei. We find that the discovery of CP violation for set-up(c) and set-up (d) are not good and could not be found even at 1σ confidence level. For longer than 250 km baselines we have not presented any plots for CP violation discovery reach. It seems one of the basic problem for longer baselines will be relatively bad energy resolution because we are trying to use vertex resolution for getting energy resolution but there is beam spreading and as such over longer baseline beam spreading will make the energy resolution poorer.

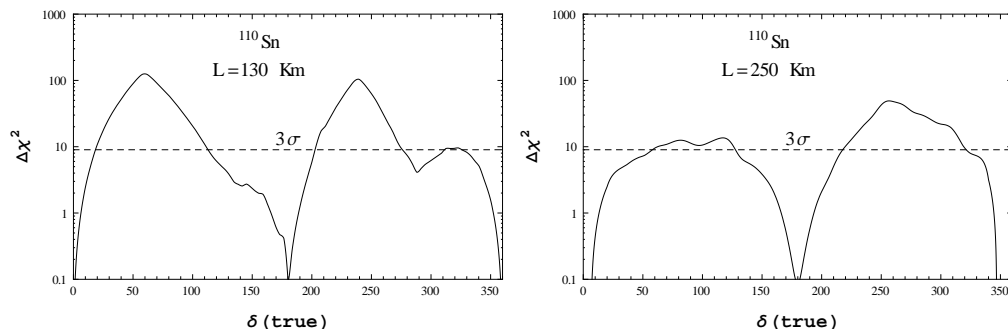


FIG. 10: $\Delta\chi^2$ versus δ (true) for two experimental set-ups (a) & (b) with nuclei ^{110}Sn for true normal hierarchy.

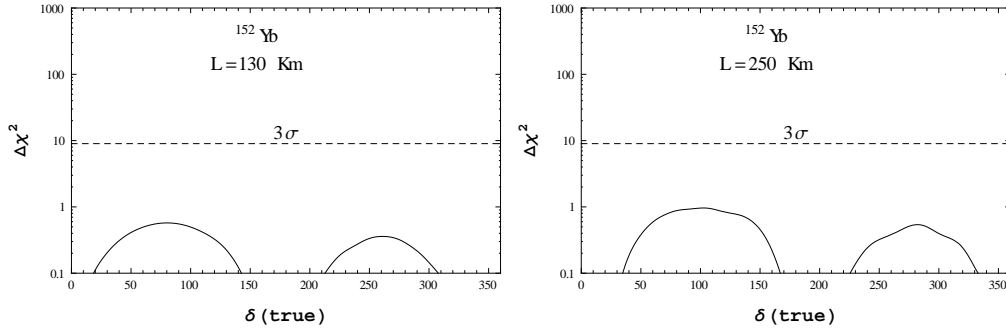


FIG. 11: $\Delta\chi^2$ versus $\delta(\text{true})$ for two experimental set-ups (c) & (d) with nuclei ^{152}Yb for true normal hierarchy.

In our analysis we have chosen neutrino energy near the oscillation peak (as shown in Figure 9) which is more δ sensitive region. This consideration improves the CP violation discovery reach. However, in [45] (as shown in Figure 7 of that paper) CP violation discovery reach has been shown to be about 81% of the possible δ values for their set-up II for 250 km baseline for the presently known θ_{13} value. The discovery reach seems to be not so good in our case although we have chosen appropriately the neutrino energy where probability of oscillation is δ sensitive. It is because in our analysis we have considered more realistic value of γ (which is lower than that considered in [45] but could be achievable at present (keeping in mind the possible SPS upgrade at CERN)). We have also taken into account the beam spreading in our present analysis in estimating effective energy resolution and have taken only a few neutrino energy bins for the analysis unlike [45] as it is important to consider the size of the energy bins larger in comparison to the level of energy resolution. Our results shows that the nuclei $^{110}_{50}\text{Sn}$ is more suitable than the nuclei ^{152}Yb so far CP violation discovery reach is concerned.

IV. CONCLUSION

We have studied the possible CP violation discovery reach due to Dirac phase δ in the leptonic sector through neutrino oscillation experiments with superbeam, neutrino factory and mono-energetic neutrino beam from electron capture process. Particularly for superbeam and neutrino factory we have studied the NSI effect on the CP violation discovery reach. However, for mono-energetic neutrino beam we have considered shorter baseline as required technically for lower boost factor γ . For that NSI effect seems to be insignificant and hence we have studied discovery of CP violation due to δ without different NSI in this case.

For short baseline with CERN-Fréjus and T2HK set-up in case of superbeam for different NSI satisfying model dependent bound we find that there is insignificant effect due to real NSI on the the discovery reach of CP violation due to δ . For longer baseline with CERN-Pyhäsalmi set-up such effects are significant. In case of neutrino factory, the baselines considered are slightly longer than those for superbeam. In this case, except $\varepsilon_{\mu\mu}$ other NSIs have significant effect on $F(\delta)$.

As $F(\delta)$ is never found to be 1, obviously for some values of δ , CP violation may not be observed at certain confidence level for the kind of detectors we have considered (see Figure 1). Even if one observes CP violation due to δ in shorter baselines there is a possibility of observing no CP violation in presence of real NSI. This feature can be seen in Figure 2 for superbeam in presence of real NSIs - ε_{ee} , $\varepsilon_{\tau\tau}$ and in Figure 6

in presence of real NSI $\varepsilon_{\tau\tau}$ for neutrino factory. For smaller values of NSI, the CP violation discovery reach is much better for neutrino factory set-ups than those for superbeam set-ups. However, if NSIs like ε_{ee} , $\varepsilon_{e\tau}$ and $\varepsilon_{\tau\tau}$ are of significant strength $\gtrsim 0.1$ then CP violation discovery reach at neutrino factory could be very bad in comparison to particularly T2HK set-up in superbeam. One interesting feature is found from Figure 2. If one does not observe CP violation due to δ in shorter baselines (say CERN-Fréjus set-up) there is still a possibility of observing CP violation in longer baselines (see CERN-Pyhäsalmi set-up with off-diagonal NSI like $\varepsilon_{e\mu}$ and $\varepsilon_{e\tau}$) which could be the signal of NSI with significant strength. Using short and long baseline one could conclusively tell about CP violation due to δ and about NSI under such situation.

NSI - $\varepsilon_{e\mu}$, $\varepsilon_{e\tau}$ and $\varepsilon_{\mu\tau}$ could be complex. We have considered the corresponding phases $\phi_{e\mu}$, $\phi_{e\tau}$ and $\phi_{\mu\tau}$ respectively in the analysis of the discovery reach of total CP violation for both in absence and in presence of δ . Even in absence of δ one may observe CP violation due to the presence of NSI phases. The possibility of observing CP violation under such scenario is relatively better in general for longer baselines for both superbeam (see Figure 3) and neutrino factory (see Figure 7) provided that absolute values of NSIs are known. For $\varepsilon_{e\mu}$ there is better CP violation discovery reach in neutrino factory set-up. For $\varepsilon_{e\tau}$ neutrino factory set-up with longer baseline is slightly better than CERN-Pyhäsalmi set-up in superbeam at 3σ . For $\varepsilon_{\mu\tau}$ there is better CP violation discovery reach for CERN-Pyhäsalmi set-up in superbeam.

Assuming that there are two sources of CP violation simultaneously existing in nature- one due to δ and the other due to say one of the NSI phases ϕ_{ij} , the total CP violation discovery reach has been shown as unshaded region in the $\phi_{ij} - \delta$ plane in Figure 4 for superbeam and Figure 8 for neutrino factory. From the Figures it is seen that for NSI - $\varepsilon_{e\mu}$ for T2HK set-up there is more allowed region and as such better discovery reach is possible in the $\delta - \phi_{ij}$ parameter space particularly in comparison to CERN-Pyhäsalmi set-up in superbeam. For NSI - $\varepsilon_{e\tau}$ and $\varepsilon_{\mu\tau}$, the discovery reach of total CP violation is better for both longer and shorter baselines (like CERN-Pyhäsalmi set-up and T2HK set-up). As compared to Figure 4 due to different superbeam set-ups, we find significantly better discovery reach of CP violation for neutrino factory set-up for 730 km baseline in Figures 8. Comparing Figures 8 and 4 we find that for $\phi_{e\tau}$ if we combine experimental data from superbeam set-ups and neutrino factory set-ups, there are scopes to improve the total CP violation discovery reach further. However, it would be difficult to disentangle the observed CP violation coming due to both δ and NSI phase. In presence of some ranges of off-diagonal NSI phase values $\phi_{e\mu}$ and $\phi_{\mu\tau}$ (see upper panel of Figure 4 for superbeam and Figure 8 for neutrino factory) there is possibility of discovering total CP violation for any possible δ_{CP} value at 3σ .

The CP violation due to δ could remain unobservable with present and near future experimental facilities in superbeam and neutrino factory for certain range of values of δ (as for example for superbeam with T2HK set-up in Figure 1 for about 0° to 25° , 160° to 208° , 340° to 360° at 3σ confidence level). However, in presence of NSIs (with or without phases) the CP violation due to δ or the total CP violation due to δ and NSI phase could be observed even for such values of δ as can be seen in various Figures shown in Section III-A and B.

Basic strategy to find CP violation in the leptonic sector in presence of NSI for superbeam set-up may be to consider both shorter baseline (say T2HK set-up) as well as one longer baseline (say CERN-Pyhäsalmi set-up) because of their complementary nature with respect to the discovery reach of CP violation. If NSI values are smaller ($\lesssim 0.1$) and real then the CP violation discovery in neutrino factory set-up with MIND detector seems significantly better than superbeam set-up. For complex NSIs, consideration of both superbeam set-up and neutrino factory set-up could give better CP violation discovery reach.

We have discussed only the possibility of discovering CP violation. However, experimentally disentangling

CP violation coming from δ present in PMNS matrix, the NSI phases and the absolute value of NSI could be very difficult. One may note that for longer baselines due to higher matter density NSI effect could be more. Also the effect due to δ and that due to NSI on oscillation probability in particular channel varies differently with neutrino energy. Only if the experimental data is available over certain range of neutrino energy from the shorter and longer baseline experiments then only the multi-parameter fit could help in disentangling effects due to different unknown parameters.

For monoenergetic neutrino beam sources we have considered two different nuclei - one ν_e source is from electron capture decays of $^{110}_{50}\text{Sn}$ isotopes and the other ν_e source is from electron capture decays of isotopes ^{152}Yb . For each case we have considered two baselines 130 km and 250 km. Among experimental set-ups (a-d) in III C we find that the set-up (a) with $^{110}_{50}\text{Sn}$ isotope and 130 km baseline is found to be the most suitable set-up for discovering CP violation with $F(\delta)$ about 51 % at 3σ confidence level.

When one considers technical issues involved in the accelerator and running the ions through vacuum tube, isotopes ^{152}Yb is better candidate than $^{110}_{50}\text{Sn}$ isotopes because of much lesser half life. ^{152}Yb is also better because of the dominant electron capture decay to one energy level. However, as can be seen from Figures 10 and 11, the discovery reach of CP violation is found to be better for $^{110}_{50}\text{Sn}$ isotopes. Out of different baselines for $^{110}_{50}\text{Sn}$ nuclei, we find slightly better discovery reach for shorter baseline of 130 km with $\gamma = 500$.

Building up of such monoenergetic neutrino beam facilities will require some technological development and the implementation of it might take some time [94]. The existing CERN accelerator complex could be used to study such facility. However, the monoenergetic neutrino flux require a very large number of ions to be stored in the decay ring. It is difficult to control the beam at high intensities because of space charge detuning, intra beam scattering and vacuum loss. With SPS upgrade it could be possible to accelerate the ions to $\gamma = 480$ but accelerating above that seems difficult [90–92]. Depending on the half life of $^{110}_{50}\text{Sn}$ we have reduced the total number of useful decays of the ion per effective year from 10^{18} but the value considered is still extreme because of the requirement of acceleration and storage of the partially charged ion. For improving this the vacuum conditions in SPS would be required to be upgraded. It requires more study on such beam facility. With technological improvement if it is possible to consider monoenergetic beam with $\gamma > 1000$ [93], then the CP violation discovery reach will improve further than what has been presented in this work.

ACKNOWLEDGMENTS

ZR thanks University Grants Commission, Govt. of India for providing research fellowships. AD thanks Council of Scientific and Industrial Research, India for financial support through Senior Research Fellowship (EMR No. 09/466(0125)/2010-EMR-I). We thank L. Whitehead and Luca Agostino for providing migration matrices for Liquid Argon detector and large scale water Cherenkov detector (as studied by MEMPHYS collaboration) respectively and for their other helpful communications. RA thanks R. Gandhi and S. K. Agarwalla for helpful discussion. We thank anonymous referee whose suggestions and comments have helped

us immensely in improving the work.

-
- [1] B. Pontecorvo, *Zh. Eksp. Teor. Fiz.* **33**, 549 (1957) and **34**, 247 (1958); Z. Maki, M. Nakagawa and S. Sakata, *Prog. Theor. Phys.* **28**, 870 (1962).
- [2] S. M. Bilenky, J. Hosek and S. T. Petcov, *Phys. Lett.* **B94**, 495 (1980); J. Schechter and J. W. F. Valle, *Phys. Rev. D* **22**, 2227 (1980); M. Doi *et al.*, *Phys. Lett. B* **102**, 323 (1981).
- [3] K. A Olive *et al.* (Particle Data Group), *Chin. Phys. C*, **38**, 090001 (2014).
- [4] Y. Abe *et al.* [Double-CHOOZ Collaboration], *Phys. Rev. Lett.* **108**, 131801 (2012), (*Preprint* arXiv:1112.6353).
- [5] F. P. An *et al.* [DAYA-BAY Collaboration], *Phys. Rev. Lett.* **108**, 171803 (2012), (*Preprint* arXiv:1203.1669).
- [6] J. K. Ahn *et al.* [RENO Collaboration], *Phys. Rev. Lett.* **108**, 191802 (2012) [arXiv:1204.0626 [hep-ex]].
- [7] K. Abe *et al.* [T2K Collaboration], *Phys. Rev. Lett.* **112**, 061802 (2014) [arXiv:1311.4750 [hep-ex]].
- [8] M. Bass *et al.* [LBNE Collaboration], arXiv:1311.0212 [hep-ex].
- [9] S. K. Agarwalla *et al.* [LAGUNA-LBNO Collaboration], *JHEP* **1405**, 094 (2014) [arXiv:1312.6520 [hep-ph]].
- [10] T. Stora, E. Noah, R. Hodak, T. Y. Hirsh, M. Hass, V. Kumar, K. Singh and S. Vaintraub *et al.*, *Europhys. Lett.* **98**, 32001 (2012).
- [11] R. Edgecock, *J. Phys. Conf. Ser.* **408**, 012011 (2013).
- [12] E. Christensen, P. Coloma and P. Huber, *Phys. Rev. Lett.* **111**, 061803 (2013), arXiv:1301.7727; T. R. Edgecock *et al.*, *Phys. Rev. ST Accel. Beams* **16**, 021002 (2013); C. Rubbia, arXiv:1306.2234; A. Dasgupta, Z. Rahman and R. Adhikari, arXiv:1210.4801; Z. Rahman, A. Dasgupta and R. Adhikari, arXiv:1210.2603.
- [13] Y. Itow *et al.* [T2K Collaboration], *Preprint* hep-ex/0106019.
- [14] J. -E. Campagne, M. Maltoni, M. Mezzetto and T. Schwetz, *J. High Energy Phys.* *JHEP* **0704**, 003 (2007), (*Preprint* hep-ph/0603172).
- [15] S. Choubey *et al.* [IDS-NF Collaboration], *Preprint* arXiv:1112.2853.
- [16] P. Zucchelli, *Phys. Lett. B* **532**, 166 (2002).
- [17] J. Bouchez, M. Lindroos and M. Mezzetto, *AIP Conf. Proc.* **721**, 37 (2004), (*Preprint* hep-ex/0310059).
- [18] P. Coloma, E. Fernandez-Martinez and L. Labarga, *J. High Energy Phys.* *JHEP* **1211**, 069 (2012), (*Preprint* arXiv:1206.0475).
- [19] P. Coloma, A. Donini, E. Fernandez-Martinez and P. Hernandez, *J. High Energy Phys.* *JHEP* **1206**, 073 (2012), (*Preprint* arXiv:1203.5651).
- [20] D. Meloni, T. Ohlsson, W. Winter and H. Zhang, *JHEP*, **04**, 041 (2010).
- [21] T. Ohlsson, *Rept. Prog. Phys.* **76**, 044201 (2013), (*Preprint* arXiv:1209.2710).
- [22] S. K. Raut, R. S. Singh and S. U. Sankar, *Phys. Lett. B* **696**, 227 (2011), (*Preprint* arXiv:0908.3741).
- [23] A. Dighe, S. Goswami and S. Ray, *Phys. Rev. Lett.* **105**, 261802 (2010), (*Preprint* arXiv:1009.1093).
- [24] S. K. Agarwalla, T. Li and A. Rubbia, *J. High Energy Phys.* *JHEP* **1205**, 154 (2012), (*Preprint* arXiv:1109.6526).
- [25] P. Coloma, T. Li and S. Pascoli, *Preprint* arXiv:1206.4038.
- [26] P. Coloma, P. Huber, J. Kopp and W. Winter, *Phys. Rev. D* **87**, 033004 (2013), (*Preprint* arXiv:1209.5973).
- [27] J. Kopp, M. Lindner, T. Ota and J. Sato, *Phys. Rev. D* **77**, 013007 (2008), (*Preprint* arXiv:0708.0152).
- [28] T. Ota, *AIP Conf. Proc.* **981**, 231 (2008).
- [29] P. Ballett and S. Pascoli, *Phys. Rev. D* **86**, 053002 (2012) [arXiv:1201.6299 [hep-ph]].
- [30] S. K. Agarwalla, P. Huber, J. Tang and W. Winter, *JHEP* **1101**, 120 (2011) [arXiv:1012.1872 [hep-ph]].
- [31] S. Geer, O. Mena and S. Pascoli, *Phys. Rev. D* **75**, 093001 (2007), hep-ph/0701258.
- [32] A. Bross, M. Ellis, S. Geer, O. Mena and S. Pascoli, *Phys. Rev. D* **77**, 093012 (2008), arXiv:0709.3889.
- [33] A. Bross, M. Ellis, S. Geer, O. Mena and S. Pascoli, *J. Phys. Conf. Ser.* **136**, 042032 (2008).
- [34] T. Li, A. Bross, M. Ellis, E. Fernandez Martinez, S. Geer, O. Mena and S. Pascoli, *AIP Conf. Proc.* **1222**, 84 (2010).

- [35] E. Fernandez Martinez, T. Li, S. Pascoli and O. Mena, *Phys. Rev. D* **81**, 073010 (2010), arXiv:0911.3776.
- [36] P. Kyberd, M. Ellis, A. Bross, S. Geer, O. Mena, K. Long, S. Pascoli and E. Fernandez Martinez *et al.*, FERMILAB-FN-0836-APC.
- [37] A. Bross, M. Ellis, S. Geer, O. Mena and S. Pascoli, *AIP Conf. Proc.* **981**, 187 (2008).
- [38] A. Bandyopadhyay *et al.* [ISS Physics Working Group Collaboration], *Rept. Prog. Phys.* **72**, 106201 (2009), arXiv:0710.4947.
- [39] J.Kopp, T. Ota and W.Winter, *Phys. Rev. D.* **78**, 053007 (2008), arXiv:0804.2261.
- [40] W. Winter, *Phys. Lett. B* **671**, 77 (2009), arXiv:0808.3583.
- [41] A. Friedland and I. M. Shoemaker, arXiv:1207.6642.
- [42] P. Coloma, A. Donini, J. Lopez-Pavon and H. Minakata, *JHEP* **1108**, 036 (2011) [arXiv:1105.5936 [hep-ph]].
- [43] International design study of the neutrino factory, <http://www.ids-nf.org/>.
- [44] A. Bross, R. Wands, R. Bayes, A. Laing, F. J. P. Soler, A. Cervera Villanueva, T. Ghosh and J. J. Gómez Cadenas *et al.*, *Phys. Rev. ST Accel. Beams* **16**, 081002 (2013), arXiv:1306.5327.
- [45] M. Rolinec, J. Sato, *JHEP* **0708**:079 (2007), hep-ph/0612148.
- [46] J. Bernabeu, J. Burguet-Castell and C. Espinoza, *JHEP*, **0512**:014 (2005), hep-ph/0505054.
- [47] J. Bernabeu, J. Burguet-Castell, C. Espinoza, and M. Lindroos, *Nucl.Phys.Proc.Suppl.* **155**, 222-224 (2006), hep-ph/0510278 .
- [48] J. Sato, *Phys.Rev.Lett.* **95**, 131804 (2005), hep-ph/0503144.
- [49] C. Orme, *JHEP* **1007**, 049 (2010), arXiv:0912.2676.
- [50] M.E. Estevez Aguado *et al.*, *Phys.Rev.* **C84**, 034304 (2011).
- [51] J. Bernabeu, J. Burguet-Castell and C. Espinoza, *PoS HEP* **2005**, 182 (2006), hep-ph/0512297.
- [52] R. Adhikari, S. Chakraborty, A. Dasgupta and S. Roy, *Phys. Rev. D* **86**, 073010 (2012), (*Preprint* arXiv:1201.3047).
- [53] C. Biggio, M. Blennow and E. Fernandez-Martinez, *J. High Energy Phys.* *JHEP* **0908** 090 (2009), (*Preprint* arXiv:0907.0097).
- [54] M. M. Guzzo, P. C. de Holanda and O. L. G. Peres, *Phys. Lett. B* **591**, 1 (2004), (*Preprint* hep-ph/0403134).
- [55] J. Barranco, O. G. Miranda, C. A. Moura and J. W. F. Valle, *Phys. Rev. D* **73** 113001 (2006), (*Preprint* hep-ph/0512195).
- [56] G. Mangano, G. Miele, S. Pastor, T. Pinto, O. Pisanti and P. D. Serpico, *Nucl. Phys. B* **756** 100 (2006), (*Preprint* hep-ph/0607267).
- [57] M. Blennow, T. Ohlsson and J. Skrotzki, *Phys. Lett. B* **660** 522 (2008), (*Preprint* hep-ph/0702059).
- [58] J. Kopp, M. Lindner and T. Ota, *Phys. Rev. D* **76** 013001 (2007), (*Preprint* hep-ph/0702269).
- [59] A. Esteban-Pretel, R. Tomas and J. W. F. Valle, *Phys. Rev. D* **76** 053001 (2007), (*Preprint* arXiv:0704.0032).
- [60] A. M. Gago, H. Minakata, H. Nunokawa, S. Uchinami and R. Zukanovich Funchal, *J. High Energy Phys.* *JHEP* **1001** 049 (2010), (*Preprint* arXiv:0904.3360).
- [61] F. J. Escrivuela, O. G. Miranda, M. A. Tortola and J. W. F. Valle, *Phys. Rev. D* **80** 105009 (2009) [Erratum-ibid. *D* **80** 129908 (2009)], (*Preprint* arXiv:0907.2630).
- [62] O. Yasuda, *Acta Phys. Polon. B* **38** 3381 (2007), (*Preprint* arXiv:0710.2601).
- [63] N. Fornengo, M. Maltoni, R. Tomas and J. W. F. Valle, *Phys. Rev. D* **65**, 013010 (2002), hep-ph/0108043.
- [64] M. B. Gavela, D. Hernandez, T. Ota and W. Winter, *Phys. Rev. D* **79**, 013007 (2009), arXiv:0809.3451.
- [65] S. Davidson, C. Pena-Garay, N. Rius and A. Santamaria, *J. High Energy Phys.* *JHEP* **0303** 011 (2003), (*Preprint* hep-ph/0302093).
- [66] G. Mitsuka *et al.* [Super-Kamiokande Collaboration], *Phys. Rev. D* **84** 113008 (2011), (*Preprint* arXiv:1109.1889).
- [67] S. Antusch, J. P. Baumann and E. Fernandez-Martinez, *Nucl. Phys. B* **810**, 369 (2009), arXiv:0807.1003.
- [68] A. Esmaili and A. Y. Smirnov, 2013 *J. High Energy Phys.* *JHEP* **1306**, 026 (2013), (*Preprint* arXiv:1304.1042).
- [69] T. Kikuchi, H. Minakata and S. Uchinami, *JHEP* **0903**, 114 (2009), arXiv:0809.3312.
- [70] H. Minakata, *Acta Phys. Polon. B* **40**, 3023 (2009), arXiv:0910.5545.
- [71] K. Asano and H. Minakata, *JHEP* **1106**, 022 (2011), arXiv:1103.4387.

- [72] A. Cervera *et al.*, *Nucl. Phys. B* **579**, 17 (2000) [Erratum-ibid. B **593**, 731 (2001)] hep-ph/0002108; E. K. Akhmedov *et al.*, *JHEP* **0404**, 078 (2004), hep-ph/0402175.
- [73] G. L. Fogli, E. Lisi, A. Marrone, D. Montanino, A. Palazzo and A. M. Rotunno, *Phys. Rev. D* **86**, 013012 (2012) [arXiv:1205.5254 [hep-ph]].
- [74] M. C. Gonzalez-Garcia, M. Maltoni and T. Schwetz, *JHEP* **1411**, 052 (2014) [arXiv:1409.5439 [hep-ph]].
- [75] A. M. Dziewonski and D. L. Anderson, *Phys. Earth Planet. Interiors* **25**, 297 (1981).
- [76] P. Huber, M. Lindner and W. Winter, *Comput. Phys. Commun.* **167** 195 (2005), (*Preprint* hep-ph/0407333).
- [77] P. Huber, J. Kopp, M. Lindner, M. Rolinec and W. Winter, *Comput. Phys. Commun.* **177**, 432 (2007), (*Preprint* hep-ph/0701187).
- [78] G. L. Fogli, E. Lisi, A. Marrone, D. Montanino and A. Palazzo, *Phys. Rev. D* **66**, 053010 (2002)[hep-ph/0206162].
- [79] L. Agostino *et al.* [MEMPHYS Collaboration], *J. Cosmology and Astroparticle Phys.* JCAP **1301**, 024 (2013), (*Preprint* arXiv:1206.6665).
- [80] P. Huber, M. Lindner and W. Winter, *Nucl. Phys. B* **645**, 3 (2002) [hep-ph/0204352].
- [81] M. Ishitsuka, T. Kajita, H. Minakata and H. Nunokawa, *Phys. Rev. D* **72**, 033003 (2005) [hep-ph/0504026].
- [82] <http://www.mpi-hd.mpg.de/personalhomes/globes/glb/SPL.html>
- [83] <http://www.mpi-hd.mpg.de/personalhomes/globes/glb/T2HK.html>
- [84] C. Adams *et al.* [LBNE Collaboration], *Preprint* arXiv:1307.7335.
- [85] L. Whitehead (Private communication).
- [86] B. Jamieson, Hyper-Kamiokande open workshop #4, Jan 28, 2014.
- [87] M. Deile [TOTEM Collaboration], hep-ex/0410084.
- [88] M. Fiorini, P. Dalpiaz, V. Guidi, G. Ambrosi, R. W. Assmann, I. Efthymiopoulos, L. Gatignon and W. Scandale *et al.*, *Conf. Proc. C* **060626**, 1538 (2006).
- [89] P. Huber, M. Lindner, M. Rolinec and W. Winter, *Phys. Rev.* **D73**, 053002 (2006), hep-ph/0506237.
- [90] C. Espinoza and J. Bernabeu, *J. Phys. Conf. Ser.* **110**, 082006 (2008), arXiv:0710.5615.
- [91] O. Bruning *et al.*, LHC luminosity and energy upgrade: a feasibility study, CERN-LHC-PROJECT-REPORT-626 (2002).
- [92] H. Bartosik *et al.*, Experimental studies for future LHC beams in the SPS, CERN-ACC-2013-0151 (2013).
- [93] P. Migliozi, A neutrino program based on the machine upgrade of the LHC, IX International conference on topics on Astroparticle and underground physics (TAUP05), Zaragoza, Spain, 10-14 September (2005).
- [94] M. Lindroos, J. Bernabeu, J. Burguet-Castell and C. Espinoza, *PoS HEP* **2005**, 365 (2006); M. Benedikt *et al.*, *Eur. Phys. J. A* **47**, 24 (2011).